NASA/CR—2004-213405

Two-Dimensional Air-Flow Tests of the Effect of ITA Flowliner Slot Modification by Grinding/Polishing on Edge Tone Generation Potential

Bruce E. Walker
Hersh Walker Acoustics, Westlake Village, California

December 2004

The NASA STI Program Office . . . in Profile

Since its founding, NASA has been dedicated to the advancement of aeronautics and space science. The NASA Scientific and Technical Information (STI) Program Office plays a key part in helping NASA maintain this important role.

The NASA STI Program Office is operated by Langley Research Center, the Lead Center for NASA's scientific and technical information. The NASA STI Program Office provides access to the NASA STI Database, the largest collection of aeronautical and space science STI in the world. The Program Office is also NASA's institutional mechanism for disseminating the results of its research and development activities. These results are published by NASA in the NASA STI Report Series, which includes the following report types:

- TECHNICAL PUBLICATION. Reports of completed research or a major significant phase of research that present the results of NASA programs and include extensive data or theoretical analysis. Includes compilations of significant scientific and technical data and information deemed to be of continuing reference value. NASA's counterpart of peer-reviewed formal professional papers but has less stringent limitations on manuscript length and extent of graphic presentations.

- TECHNICAL MEMORANDUM. Scientific and technical findings that are preliminary or of specialized interest, e.g., quick release reports, working papers, and bibliographies that contain minimal annotation. Does not contain extensive analysis.

- CONTRACTOR REPORT. Scientific and technical findings by NASA-sponsored contractors and grantees.

- CONFERENCE PUBLICATION. Collected papers from scientific and technical conferences, symposia, seminars, or other meetings sponsored or cosponsored by NASA.

- SPECIAL PUBLICATION. Scientific, technical, or historical information from NASA programs, projects, and missions, often concerned with subjects having substantial public interest.

- TECHNICAL TRANSLATION. English-language translations of foreign scientific and technical material pertinent to NASA's mission.

Specialized services that complement the STI Program Office's diverse offerings include creating custom thesauri, building customized databases, organizing and publishing research results . . . even providing videos.

For more information about the NASA STI Program Office, see the following:

- Access the NASA STI Program Home Page at ***http://www.sti.nasa.gov***

- E-mail your question via the Internet to help@sti.nasa.gov

- Fax your question to the NASA Access Help Desk at 301–621–0134

- Telephone the NASA Access Help Desk at 301–621–0390

- Write to:
  NASA Access Help Desk
  NASA Center for AeroSpace Information
  7121 Standard Drive
  Hanover, MD 21076

NASA/CR—2004-213405

Two-Dimensional Air-Flow Tests of the Effect of ITA Flowliner Slot Modification by Grinding/Polishing on Edge Tone Generation Potential

Bruce E. Walker
Hersh Walker Acoustics, Westlake Village, California

Prepared under S40405

National Aeronautics and
Space Administration

Glenn Research Center

December 2004

Available from

NASA Center for Aerospace Information
7121 Standard Drive
Hanover, MD 21076

National Technical Information Service
5285 Port Royal Road
Springfield, VA 22100

Available electronically at http://gltrs.grc.nasa.gov

Two-Dimensional Air-Flow Tests of the Effect of ITA Flowliner Slot Modification by Grinding/Polishing on Edge Tone Generation Potential

Bruce E. Walker
Hersh Walker Acoustics
Westlake Village, California 91361

Introduction

Hersh Walker Acoustics (HWA) has performed a series of wind tunnel tests to support crack-repair studies for ITA flowliner vent slots. The overall goal of these tests and is to determine if slot shape details have a significant influence on the propensity of the flowliner to produce aero-acoustic oscillations that could increase unsteady stresses on the flowliner walls.

The test series, conducted using a full-scale 2D model of a six-slot segment of the 38 slot liner, was intended to investigate the effects of altering slot shape by grinding away cracked portions.

Background

The fuel line core, upstream bellows cavity and downstream bellows cavity form a complex coupled acoustical system that may be thought of as a circular duct surrounded by two annular cavities. The two annuli are coupled to the core duct via the cascades of vent slots. The annuli are coupled to each other via the overhanging joint gap. The upstream annulus is also coupled to the core duct via the joint gap. In a swirling flow environment, aeroacoustic feedback across the width of the slots results in oscillation of the shear layer at a velocity-dependent preferred frequency. When this frequency is close to a natural resonance of the duct-bellows acoustic system (generally near the cutoff frequency of one of the propagation modes in the duct), the strong acoustic field acts to organize the oscillations in the slot shear layers so that energy is extracted from the swirling flow and converted into high intensity oscillation that may place high stresses on the structure. It is therefore a concern that increasing slot sizes or smoothing their edges might increase the coupling between duct modes and bellows cavity resonances and/or reduce flow losses near the slots and increase oscillation amplitudes.

Test Environment

Tests were conducted in the HWA wind tunnel, which incorporates the following features:

- Test Section dimensions 5 x 10 inches cross section, 24 inches long
- Variable frequency drive flow speed control, 5 m/s minimum to 80 m/s maximum in 0.13 m/s steps.
- Nearly anechoic boundaries on three sides.
- Variable incidence angle turntable for specimen mounting on fourth side.
- Pairs of ¼-inch microphones on the test section wall across from the specimen and downstream of the specimen, allowing specimen radiation measurement with boundary layer noise suppression.

2D Liner Segment Tests

Rapid-prototype plastic models of the flowliner cross-section, flattened out into a 6-inch wide, 9.75-inch long plate with full scale modeling of the bellows, slots (6 ea upstream and downstream) and overhang joint were provided by NASA. The model was trimmed and mounted on a 10-inch diameter turntable in the side of the wind tunnel. The distance from the test section side wall to the nearest slot varied from 1.25 to 2.25 inches depending upon orientation angle. The minimum distance is approximately 5 times the boundary layer thickness and sidewall effect on flow is not significant. With this arrangement, swirl and axial flow combinations could be approximated by adjusting the tunnel flow speed and the orientation angle of the specimen. It is a simplified approximation in that flow across the upstream and downstream slots are the same in the tests whereas in the actual flowliner environment, swirl and back flow have been determined to be significantly dependent upon distance from the fuel pump impeller.

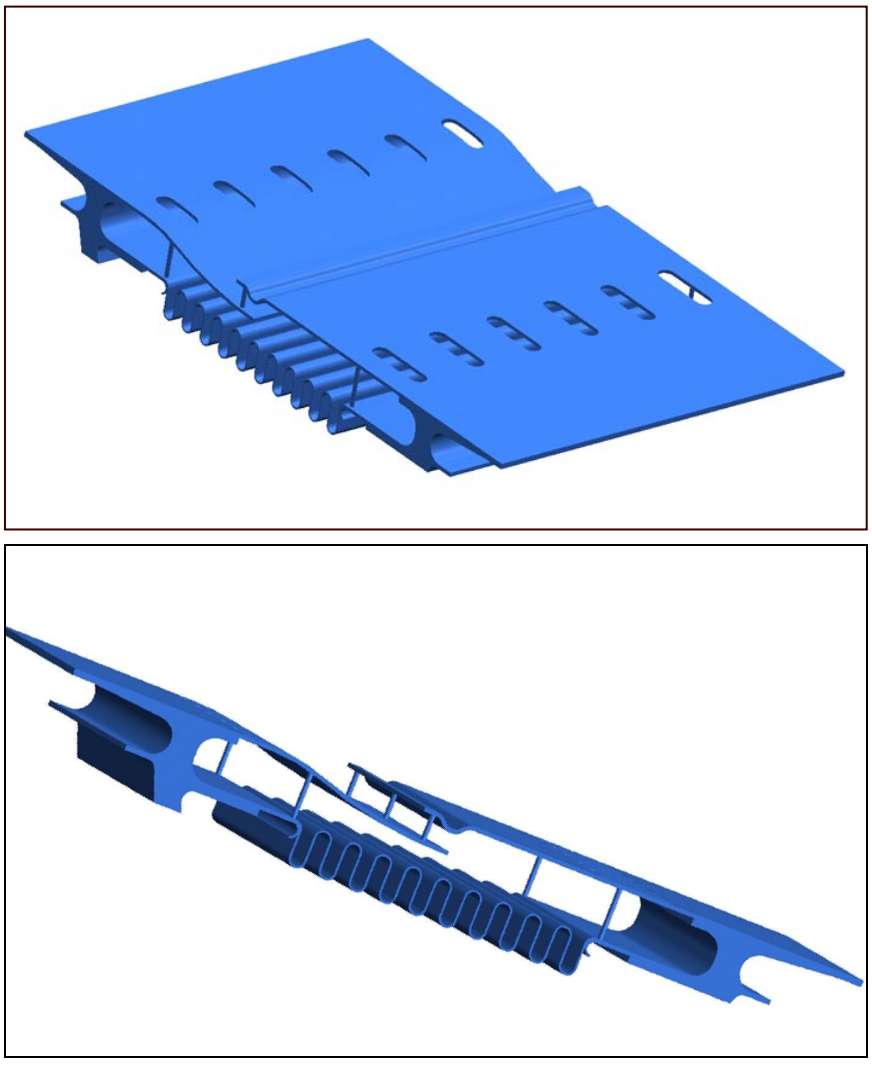

Figure 1. Isometric Views of 2D Model of Full-Scale Flowliner Segment

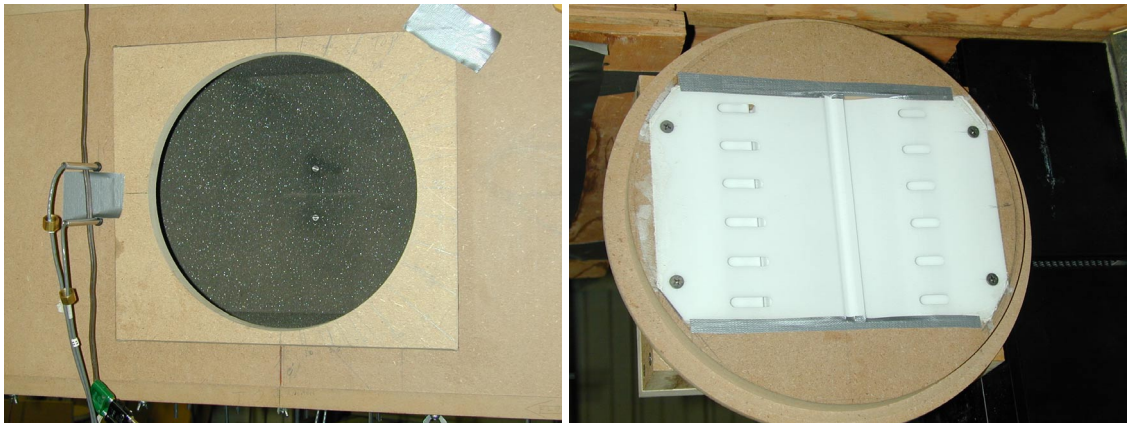

Figure 2. Photos of 2D Model and Turntable Mount in Wind Tunnel Test Section

Initial tests of the 2D liner segment model were undertaken to locate flow-induced resonances. Probe microphones were inserted near the centers of the upstream and downstream "cavities" and self-noise spectra were measured as functions of specimen orientation angles 0 to 90 degrees (purely axial flow to 100% swirl) and flow speeds 5 to 50 meters per second.

The self-noise response of the model was shown to be a complex function of flow speed and angle. As shown in the spectrogram of Figure 3, at high swirl angle (90 degrees), noise at relatively low velocities (up to 12-15 m/s) is highest in the upstream cavity at frequencies considered to be below those of interest relative to 3D measurements in LH2 and Air environments. From 15-22 m/s, 500-700 Hz tones in the downstream cavity are observed. At higher flow speeds (30-40 m/s) 1700 Hz tone noise in the downstream cavity predominates but is observed in the upstream cavity as well.

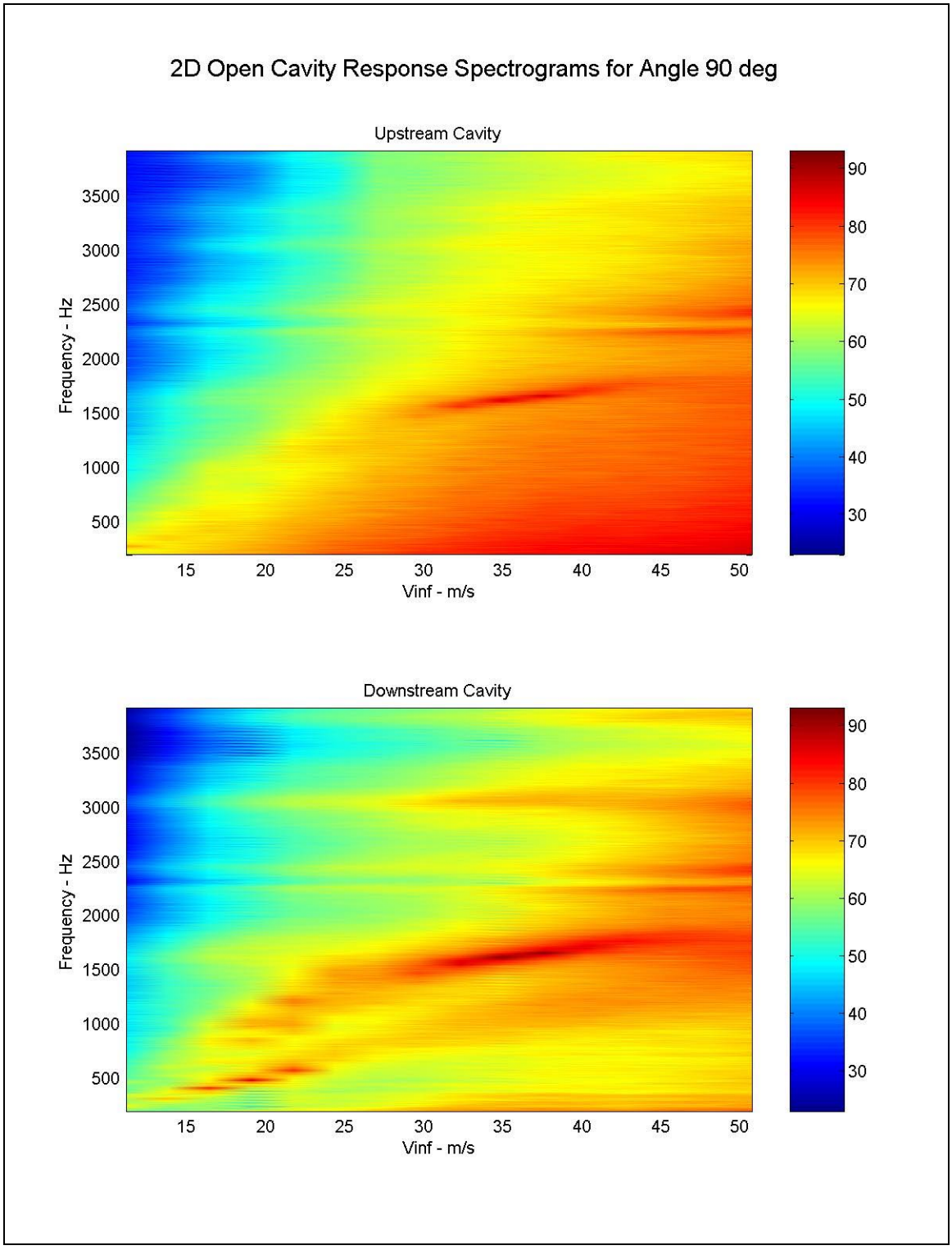

Figure 3. Baseline Spectrogram Examples

Slot Modification Test Parameters

At the time the tests were conducted, most observed cracks were in the downstream portion of the upstream slots. To investigate the potential effect of altering upstream slot shapes on self-noise amplitudes, probable flow speeds and directions were obtained for the 104.5% operating point condition near the flowliner wall at axial positions near the upstream and downstream slots. Initially, average flow conditions were provided for axial positions shown in Table 1 and illustrated in Figure 4.

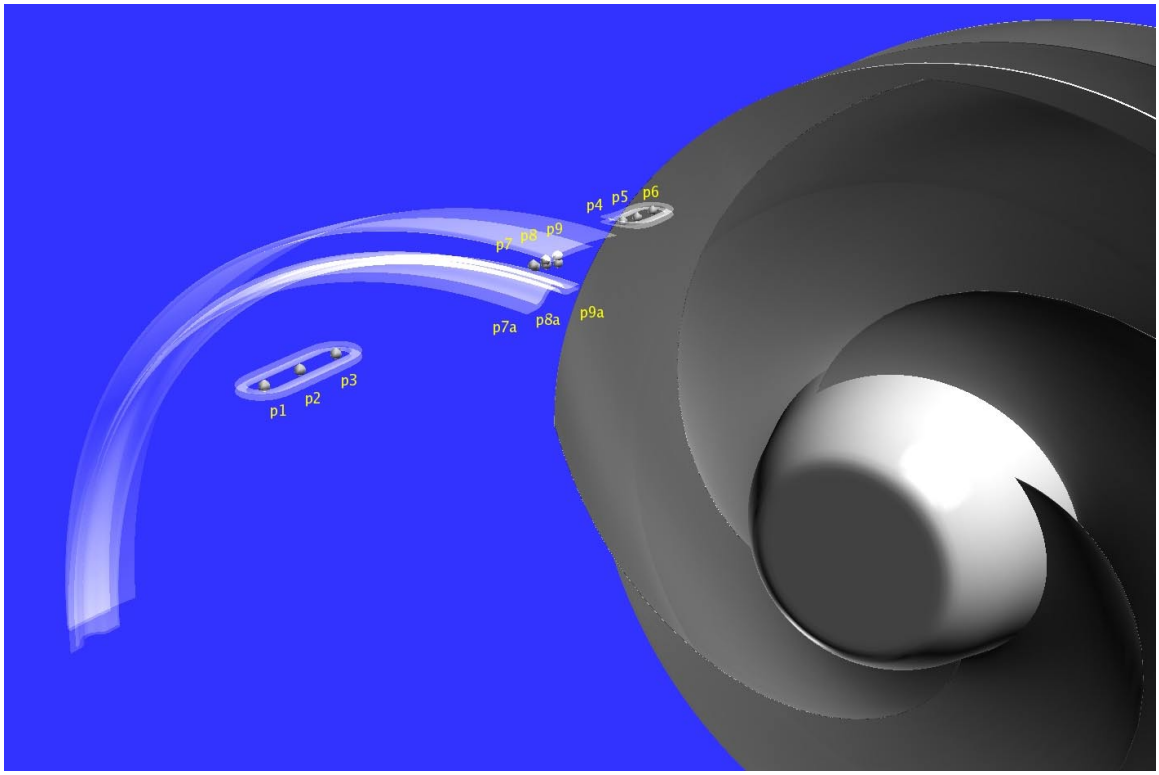

Figure 4. Illustration of Mean Flow Calculation Positions

Table 1. Flow Conditions Near Flowliner Surface Scaled to Air by Mach Number

LOCATION	Axial	Swirl	Speed	Angle
	m/s	m/s	m/s	deg
Average Flow across Upstream Slot	-0.2	-6.04	6.04	92
Average Flow across Downstream Slot	-3.07	-9.58	10.06	108
Average Flow across centers of both slots	-1.17	-7.64	7.73	99
Average Flow across both slots	-1.64	-7.81	7.98	102
Average Flow at overhang between liners	-7.1	-7.63	10.43	133
Average across both flowliners	-4.37	-7.72	8.87	120
Upstream Slot 1/8-inch from Wall	-2.74	-5.94	6.54	115
Downstream Slot 1/8-inch from Wall	-8.35	-13.7	16.05	121

To concentrate on upstream slots, it was judged appropriate to scale to the air environment by maintaining approximately constant Mach number (based on 3:1 sound speed ratio) and thus flow speeds of 7 and 11 meters per second were tested, with incidence angles ranging from 90 to 100 degrees. The two final points, computed at

1/8-inch from the flowliner wall near the slots, were provided subsequent to the testing and are listed for purposes of illustration.

To gain a better understanding of the sound pressure distribution, the 2D model was instrumented with 10 pressure microphones. Two of the microphones were flush in the surface of the central webs in the upstream and downstream slot arrays. The remaining eight were distributed in the upstream and downstream cavities. One objective was to assess the sound pressure differential across the webbing, which would impose an oscillatory stress.

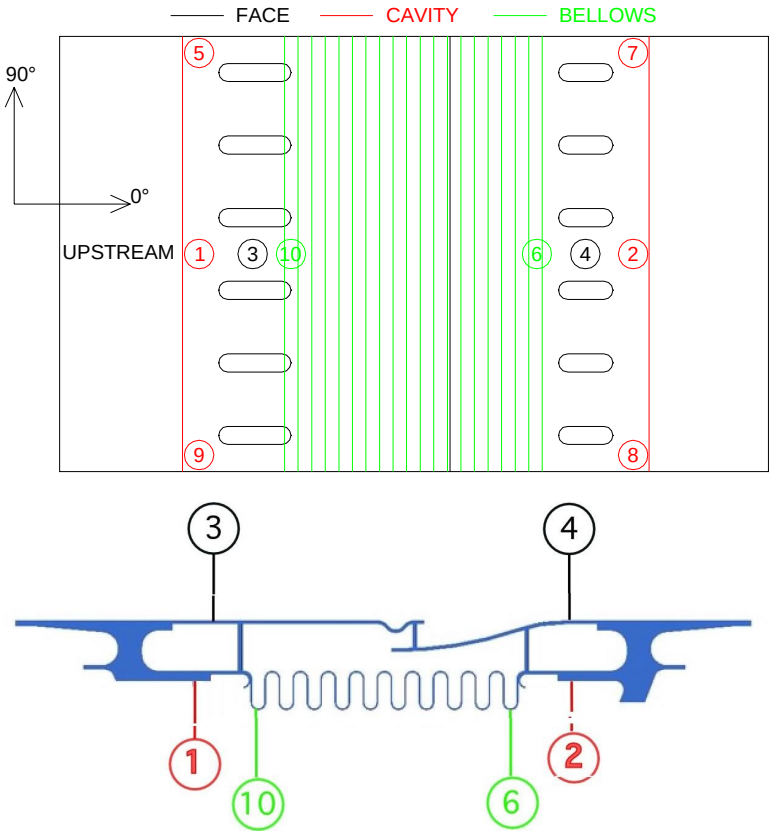

Figure 5. X-ray Top View and Section of 2D Test Model Showing Microphone Locations

Upstream Slot Configurations

Baseline configuration of the upstream slots are 1.0 inch long, 0.25 inch wide ovals with 0.125 radius round ends. Modifications tested are, in cumulative order:

A: Downstream end of the slot just "upstream" (in swirling flow) of the instrumented central web extended 35 mils (25 mils intended).

B: Downstream end of all remaining slots extended 25 mils.

C: Downstream end of the slot just "upstream" (in swirling flow) of the instrumented central web extended 80 mils (50 mils intended).

D: Downstream end of all remaining slots extended 50 mils.

E: Slot just “upstream” (in swirling flow) of the instrumented central web ground approximately 70 mils to the side to represent circumferential crack removal.

F: Slot just “upstream” (in swirling flow) of the instrumented central web extended 50 mils in all directions.

G: Two additional slots upstream of the central web extended 50 mils in all directions.

Photos of the test model in condition E and a close-up of the side-ground slot are shown in Figure 6 below.

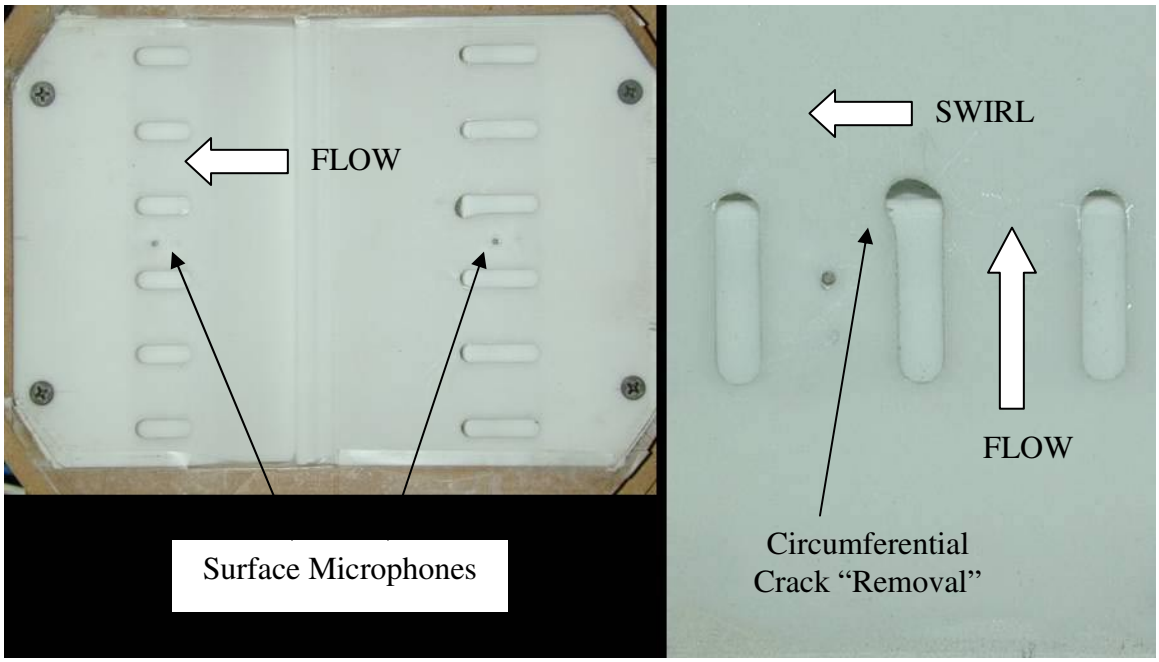

Figure 6. Photos of 2D Test Model with Upstream Slots Modified to Condition E.

Measurements

For each configuration 16 channels of measurement data were taken at the following locations and parameters:

- Channels 1 & 2: 800 Hz 1 V p-p Reference signal for frequency and timing verification
- Channels 3 – 12: 2D Model microphone signals 1 – 10 per Figure 4
- Channels 13 & 14: Flush microphones in test section wall 7 inches downstream of the model center
- Channels 15 & 16: Flush microphones in test section wall 5 inches across from the model center
- Sampling Rate: 25 kHz
- Sample Length: 2^{18} (10.5 sec)
- Inter-channel delay: 2.5 μsec per channel (1.8 deg for 2 channels at 1 kHz)

Signal Processing

To establish relationships between signals at the various sensor locations, a correlation processing technique was employed.

$$P_{a,b}(\tau) = \frac{1}{N}\sum_{i=1}^{N} p_a(t_i)\, p_b(t_i - \tau)$$

Autocorrelations ($b = a$) were computed for each signal and cross correlations were computed (at first) for each pair of signals. To provide a frequency resolution of approximately 5 Hz, delay parameter τ is required to span 0.2 seconds or 5,000 samples at 25 kHz sampling rate. As a compromise, to keep processing time manageable and to make subsequent Fourier transforms more efficient, a 4096 point (-2048 to +2047) point range was selected for τ, for a 6 Hz frequency resolution.

Frequency spectra were computed as Fourier transforms of the autocorrelations (psd) and cross correlations (cross power). Additional calculations were done to compute the cross-spectral amplitude and phase and the face-to-cavity transfer function gain and phase for selected conditions.

Test Results

Initial measurements were taken at incidence angles 97 and 99 degrees over a flow speed range 6 to 14 m/s. Cross correlations were observed between face and cavity microphone signals. These were noted to be strongly periodic as shown in Figure 7 below. Further, and more interestingly, the cross-correlations at time 0.0 were very near a negative peak, indicating 180° phase between face and cavity and oscillating slot flow as the source.

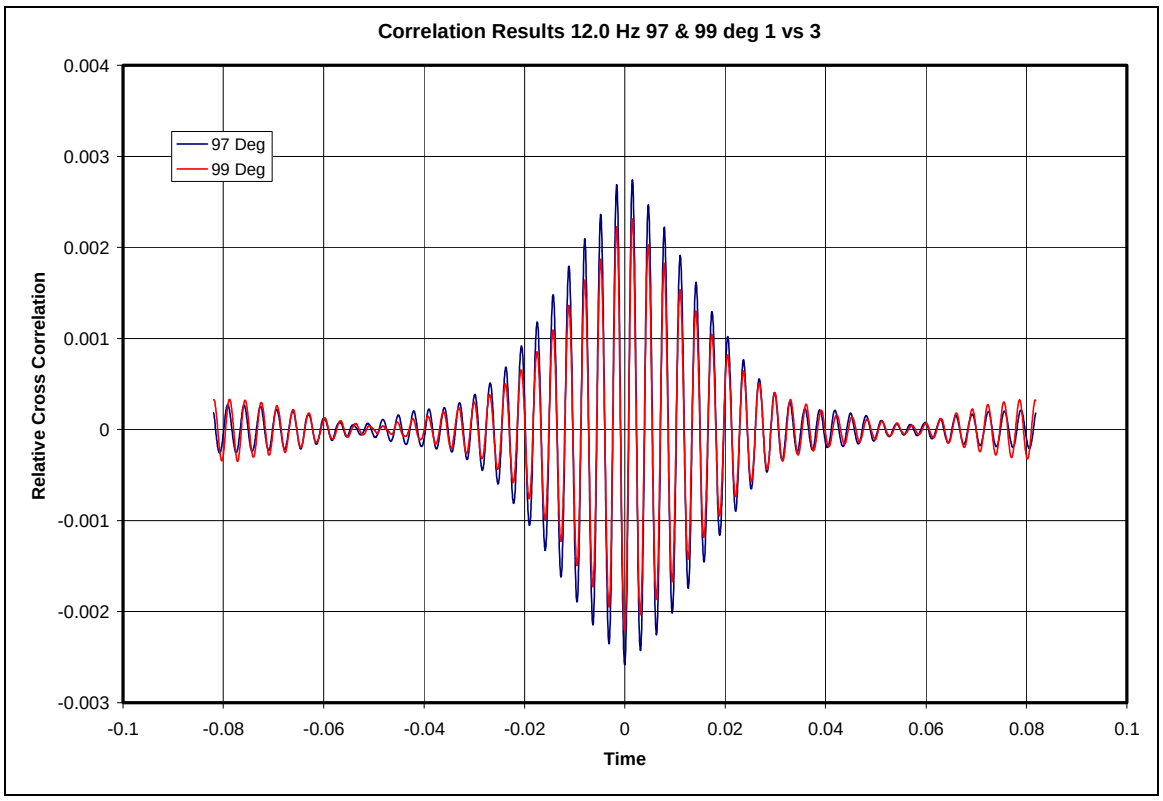

Figure 7. Cross Correlation Example Between Face and Cavity Microphones Near Center of Upstream Liner Segment

Spectral peak frequencies for upstream and downstream cavities were plotted as a function of flow velocity, with result as shown in Figure 8. Linear regression is indicative of a Strouhal number ($Nst \equiv Fd/V$), based on slot width, of 0.14 at the upstream slots and 0.072 at the downstream slots. These frequencies are puzzlingly low and were further investigated by setting the flow velocity and varying the model orientation angle.

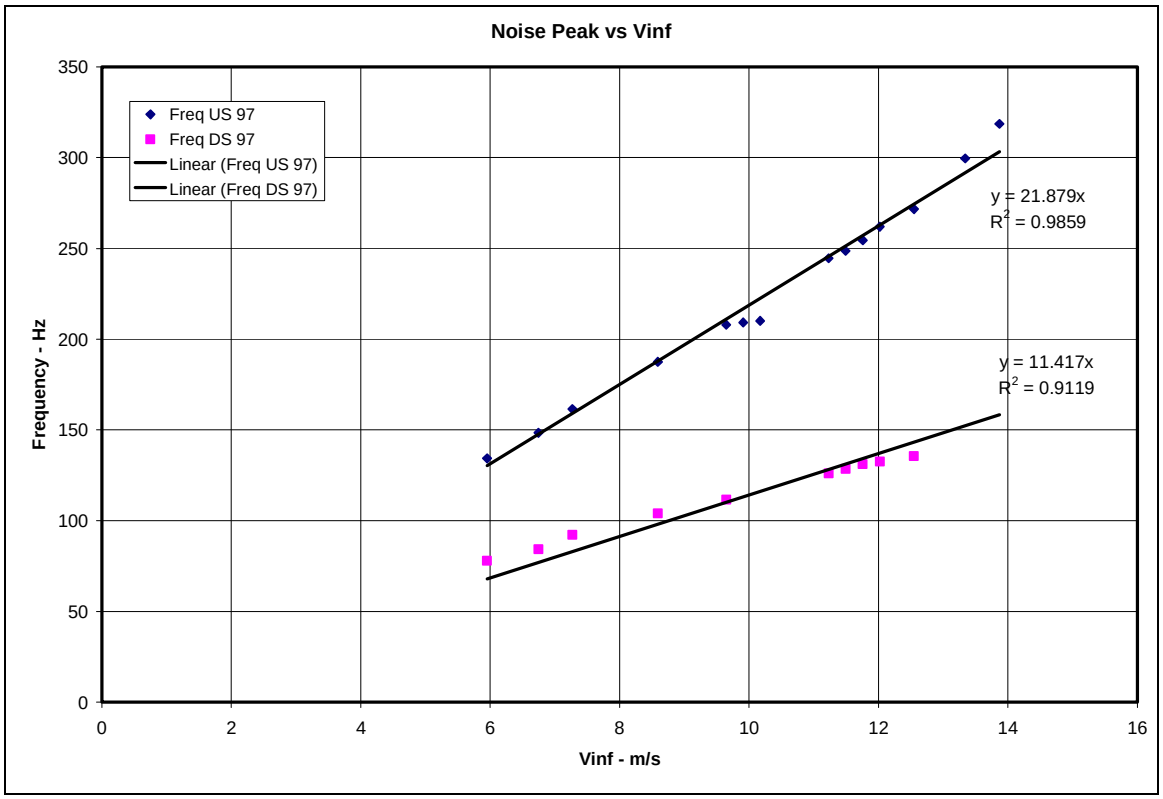

Figure 8. Spectral Peak vs Flow Speed at 97 deg Orientation Angle

Figures 9 and 10 show the effect of varying flow angle on peak response Nst at 7 m/s and 11.2 m/s flow speed respectively. Note sudden transitions at 75° and 61° for upstream and at 90° and 87° for the downstream liner segments. Note also that even at lower incidence angles, Nst is only about 0.2.

Complementing the frequency vs angle plots, Figures 11 and 12 show the relative amplitude response of the pressure differential across the slot webbing vs flow direction for the two speeds.

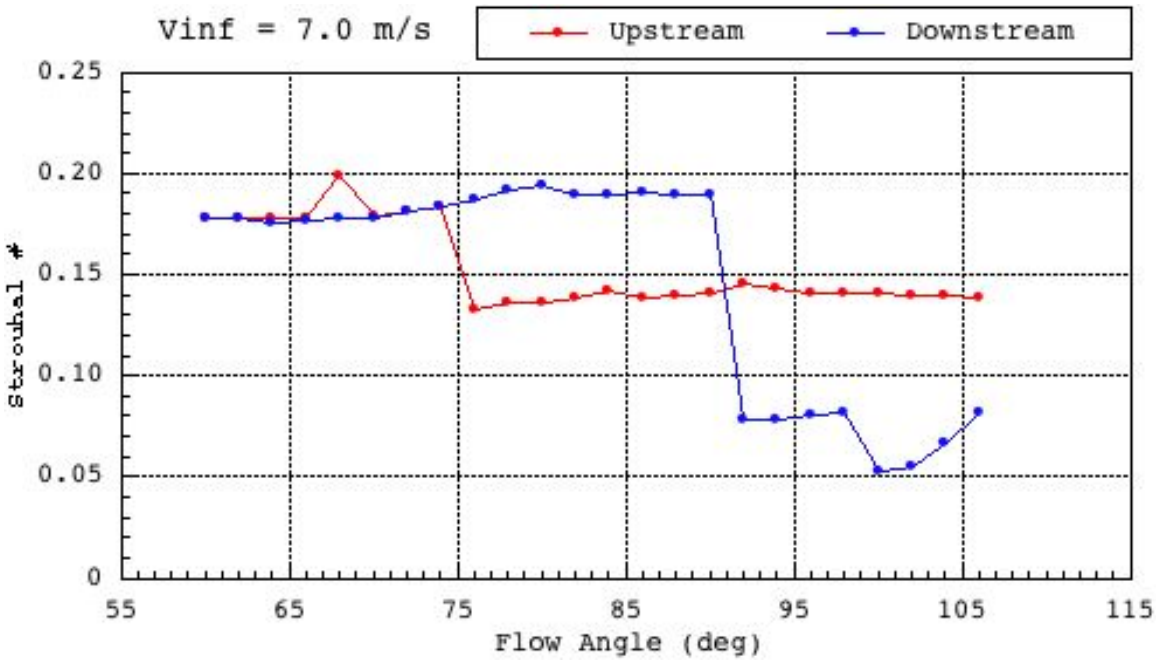

Figure 9. Strouhal Number vs Flow Angle at 7 m/s

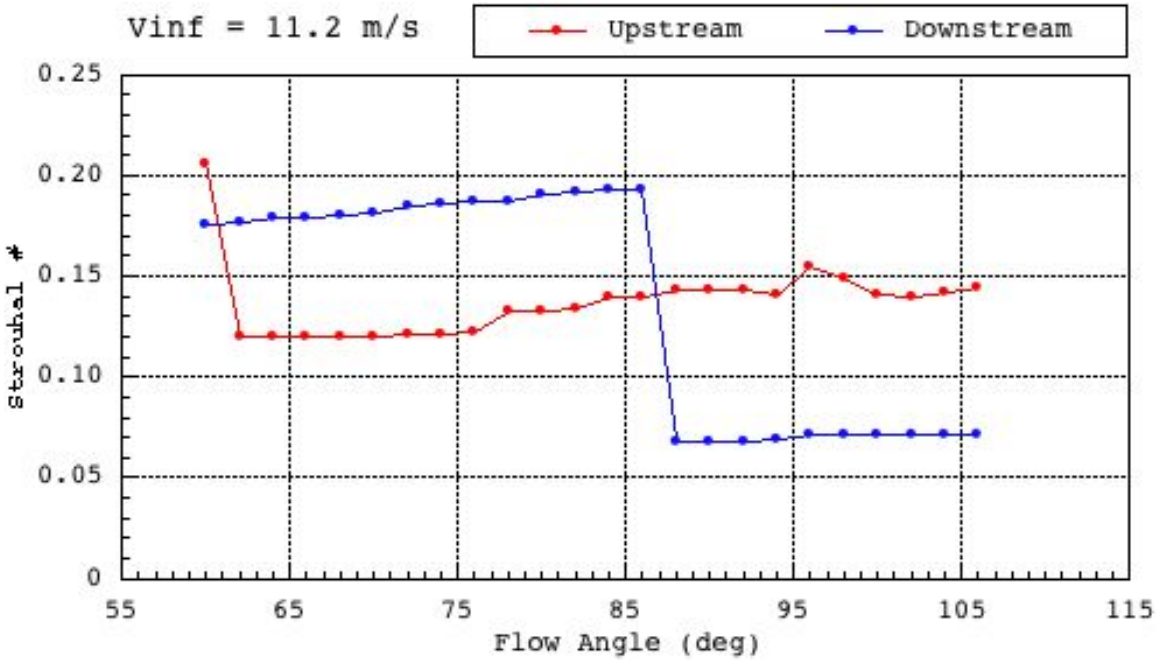

Figure 10. Strouhal Number vs Flow Angle at 11.2 m/s

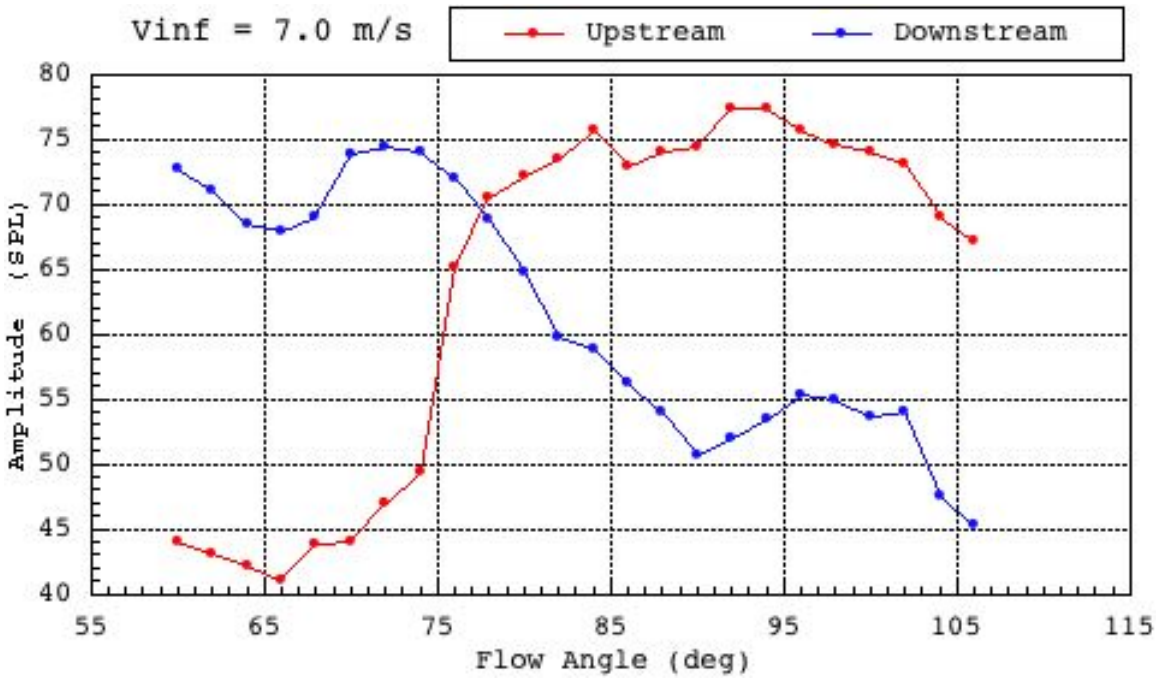

Figure 11. Peak Frequency Cross Power SPL vs Flow Angle at 7 m/s

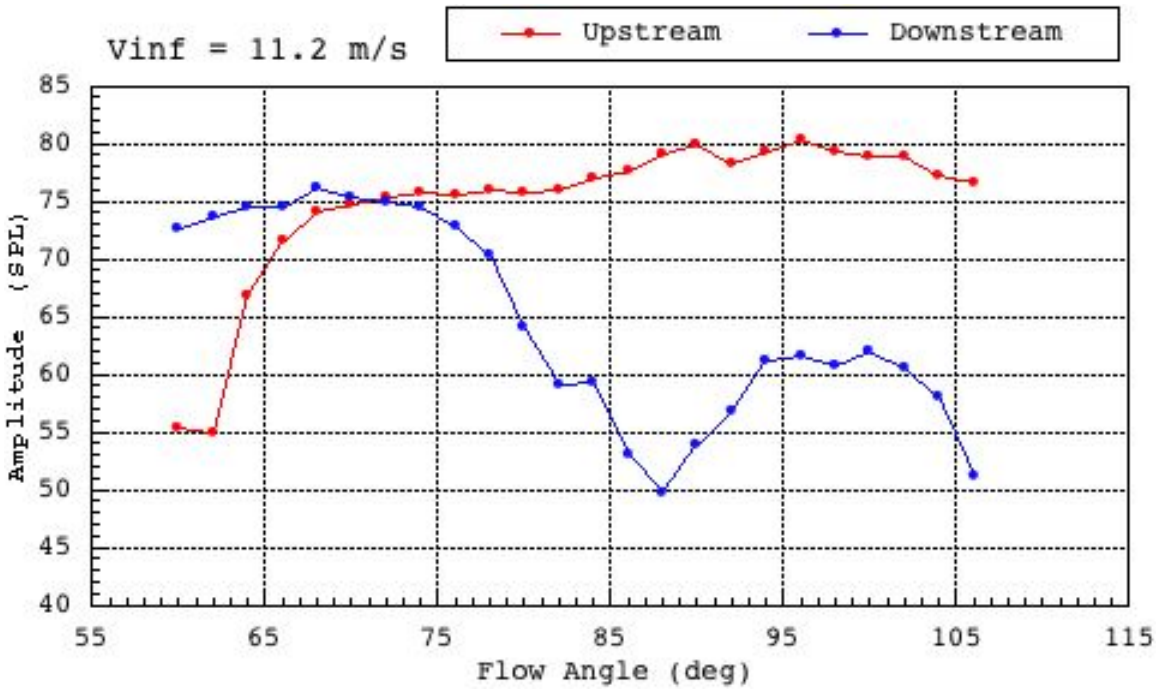

Figure 12. Peak Frequency Cross Power SPL vs Flow Angle at 11.2 m/s

In an attempt to understand the obviously complex acoustical response behavior of the 2D flowliner segment model, selected correlations and spectra from the interior of the upstream and downstream cavities were examined.

Figures 13 - 32 show, for the baseline 2D test segment model, auto and cross correlations and accompanying spectra for Upstream cavity microphones 1, 5 and 9 and Downstream cavity microphones 2, 7 and 8. The figures are included mainly to illustrate the sensitivity of response to flow conditions. Organization of the graphs is as indicated in Table 2.

Table 2. Correlation Plot Layout

Auto Correlations		Cross Correlations	
P11	P55	P15	P19
P99	P22	P59	P27
P77	P88	P28	P78

Relative to the flow, microphones 1 and 2 are in the center, microphones 8 and 9 are upstream and microphones 5 and 7 are downstream in each cavity. For discussion purposes, uppercase letters "U" and "D" refer to the designated locations and lower case "u" and "d" refer to locations relative to the flow.

Figures 13 - 16: Low swirl angle 60°

Upstream cavity pressures are a superposition of persistent 312, 362 and 30 Hz narrow band signals, in phase across cavity width.

Downstream cavity pressures feature stronger 312 Hz and 362 Hz signals dominant at upstream and downstream ends respectively, summing to produce the modulated signal at the center. Note the similarity between the P22 and P78.

Broadband noise (spike at $t = 0$) is highest at the downstream end of each cavity, possibly indicating cascade effect on flow.

Figures 17 - 20: Higher swirl angle 80°

Upstream cavity dominated by persistent 233 Hz signal, in phase across cavity width, strongest at center, weak at upstream end and 95% masked by broadband noise at downstream end.

Downstream cavity dominated by 343 Hz signal, strongest at center and downstream ends.

Cross-correlation skewed in Downstream cavity, indicating signal delay at downstream end.

Figures 21- 24: 100% swirl angle 90°

Upstream cavity dominated by damped 255 Hz signal, strong and in phase in upstream half of the cavity, weak and possibly phase reversed in the downstream end.

Virtually no tonal response in Downstream cavity.

Skewed cross correlations suggest approximately 15 ms delayed upstream to downstream response in the Upstream cavity. Note that the specimen width is 6 inches or roughly 0.15 meters. At the 11.2 meter/sec tunnel velocity, the convection time for a disturbance at an upstream slot to reach the downstream end would therefore be about 14 ms, which is consistent with the data suggesting that the quasi-periodic disturbances are convected rather than acoustically transmitted down the slot cascade.

Figures 25 - 28: Moderate reverse flow with swirl angle 96°

Upstream cavity dominated by damped 275 Hz signal, strong and in phase in upstream half of the cavity, weak and approx 90° out of phase in the downstream end.

Downstream cavity displays 275 Hz signal at reduced level.

Less skew in cross correlation than 90° case

Figures 29- Figure 32: Stronger reverse flow with swirl angle 106°

Upstream cavity dominated by damped 255 Hz signal, strong and in phase in upstream half of the cavity, weak but in phase in the downstream end.

Very weak tone response in Downstream cavity

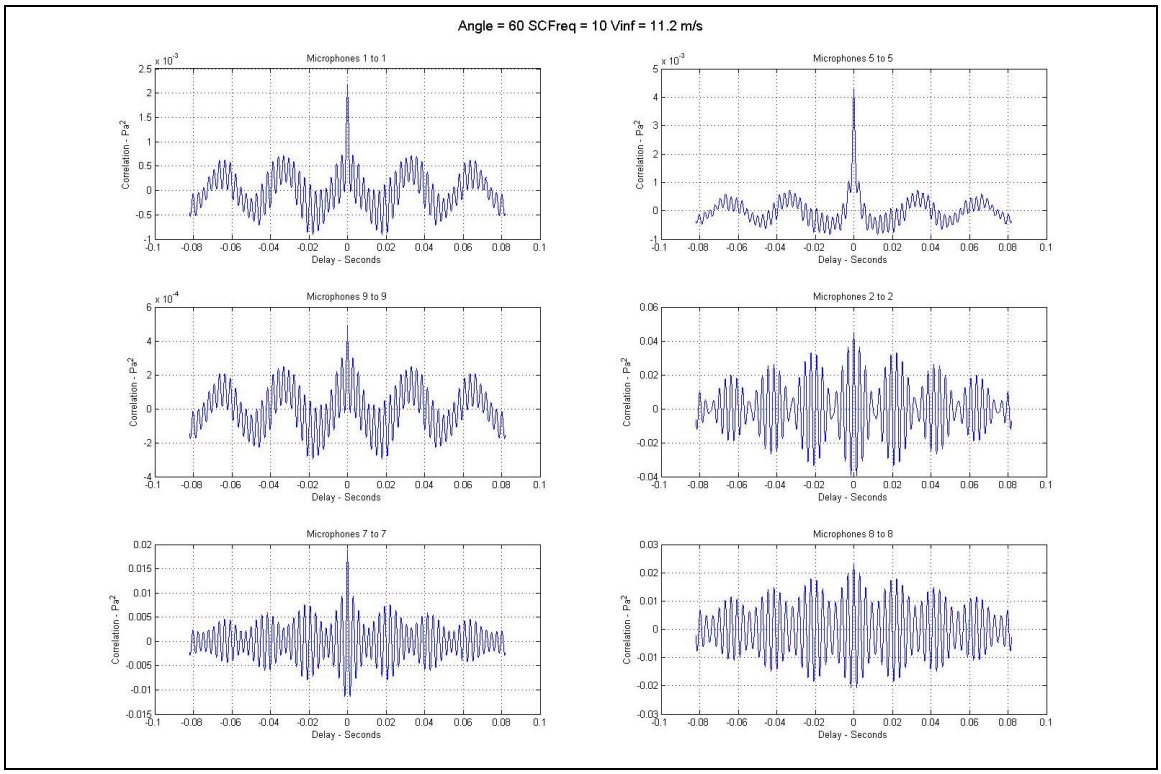

Figure 13. Cavity Auto Correlations 11.2 m/s 60 degrees

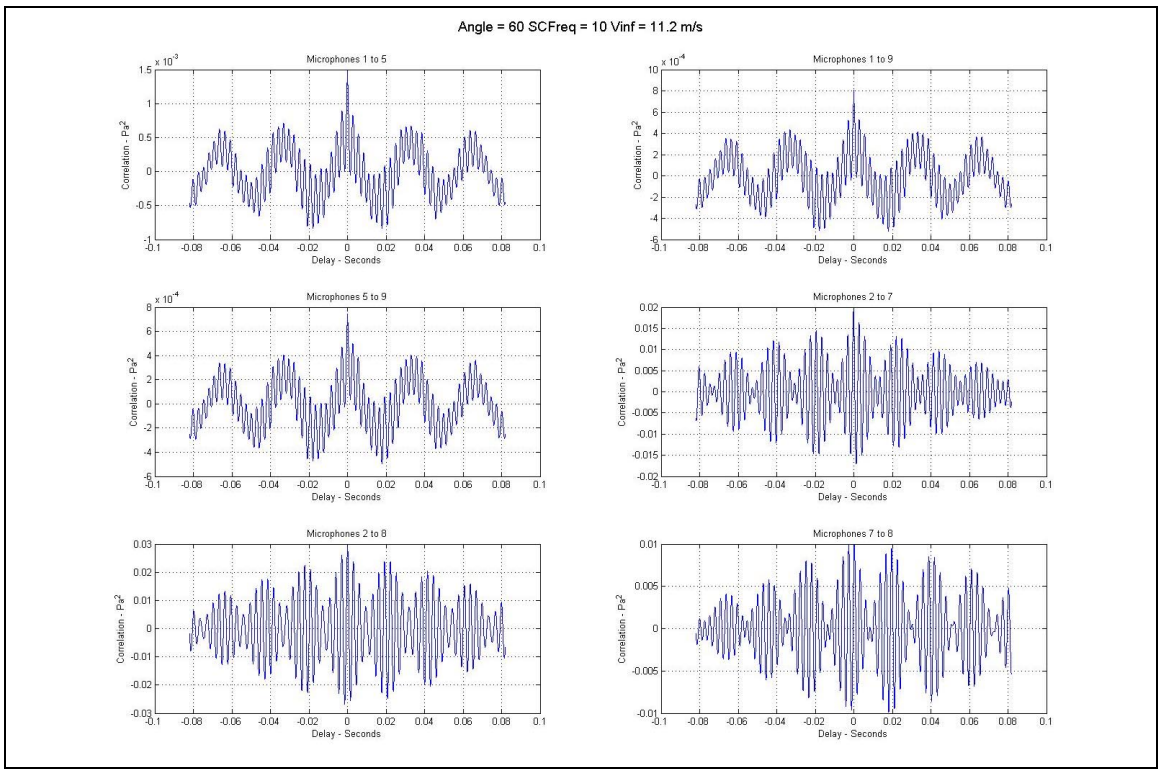

Figure 14. Cavity Cross Correlations 11.2 m/s 60 degrees

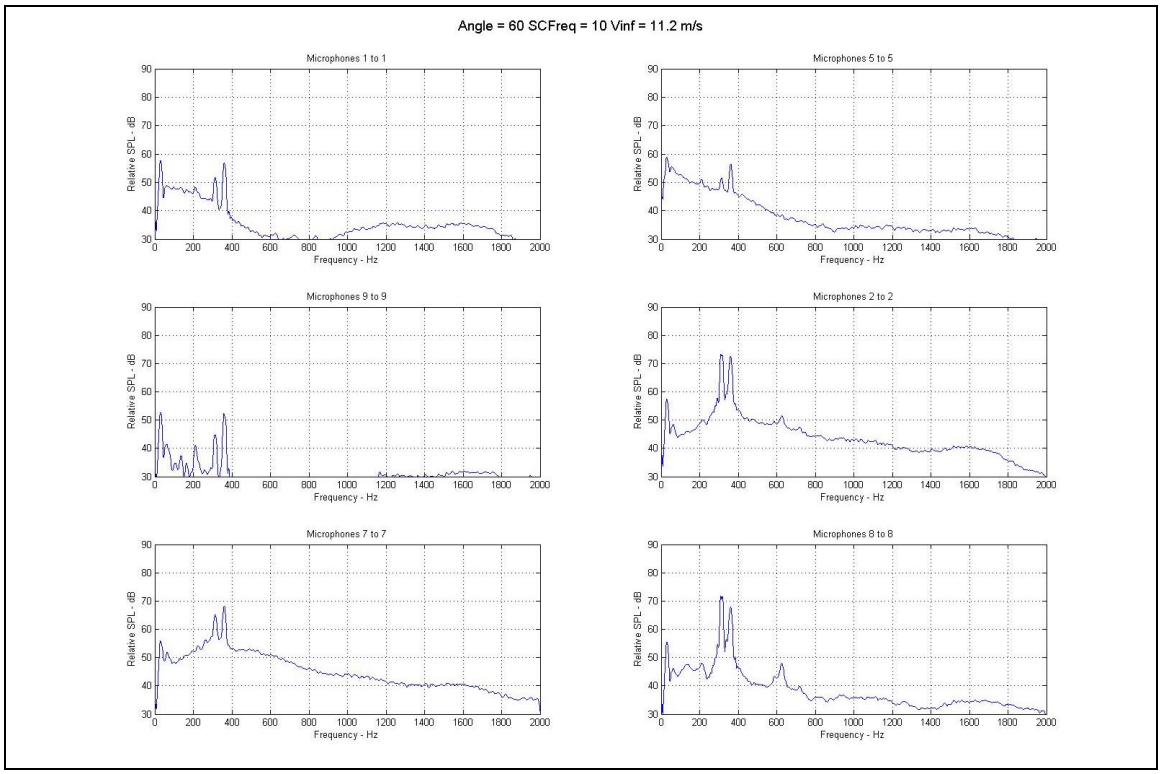

Figure 15. Cavity Auto Spectra 11.2 m/s 60 degrees

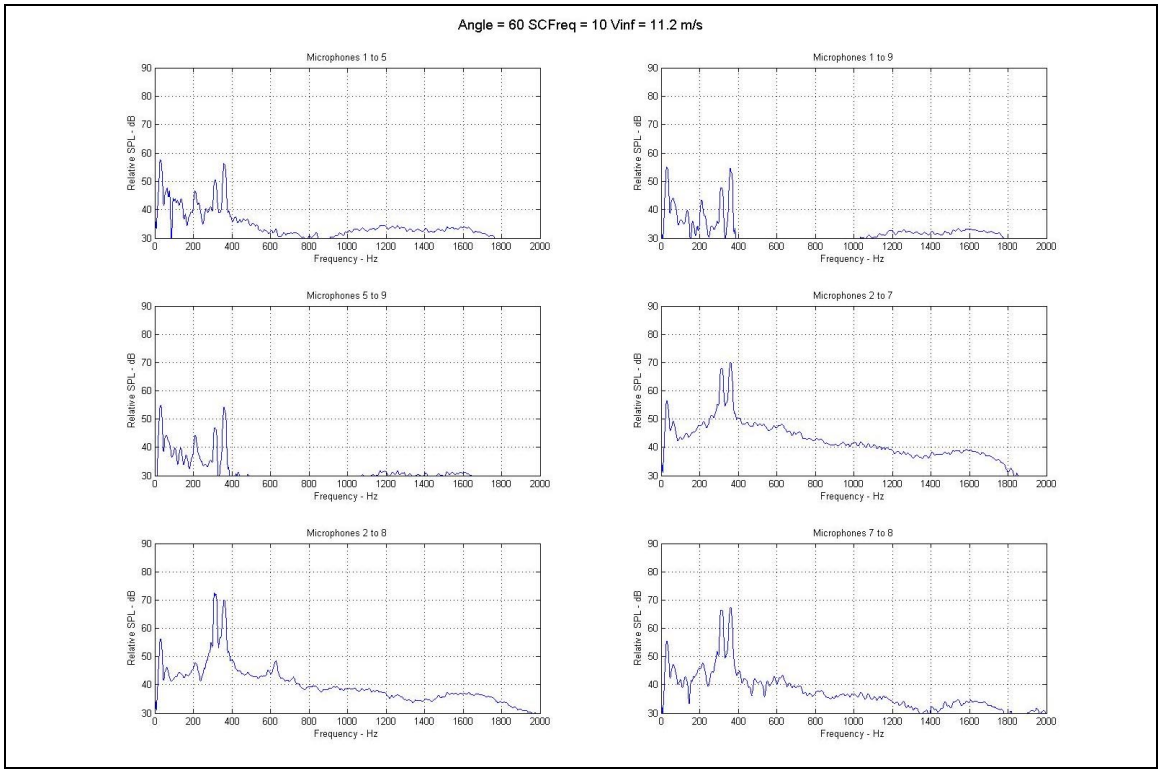

Figure 16. CavityCross Spectra 11.2 m/s 60 degrees

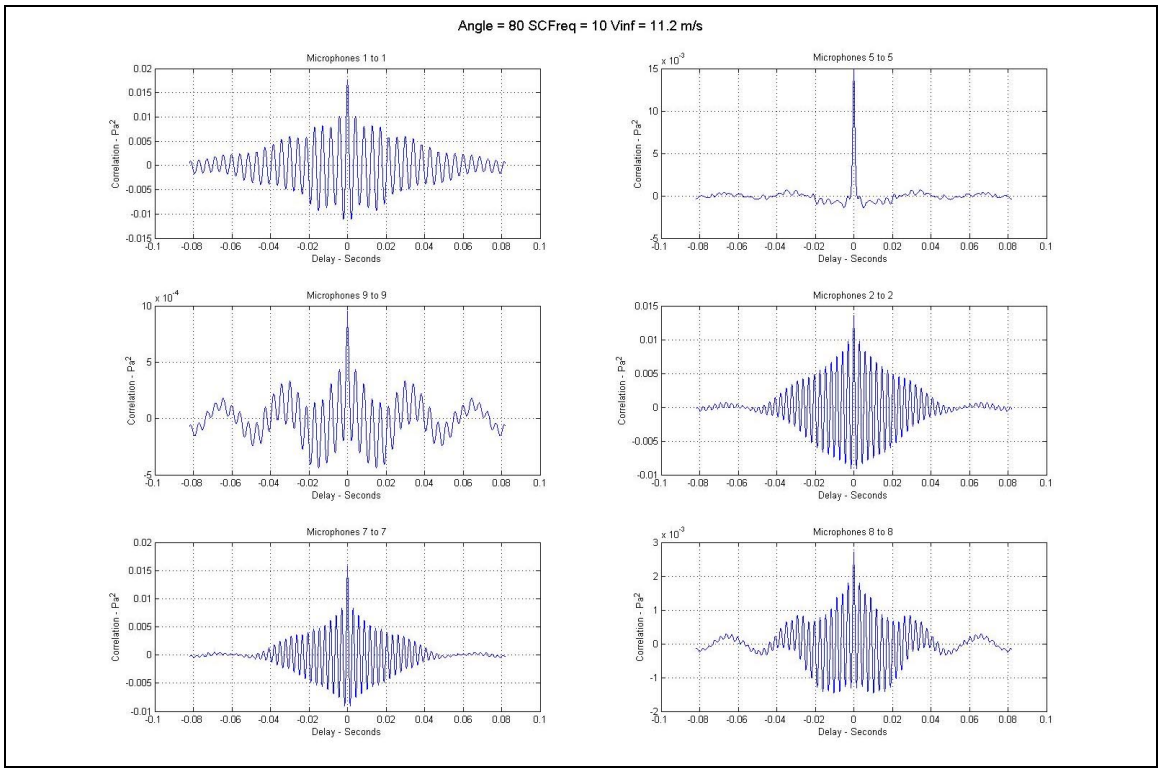

Figure 17. Cavity Auto Correlations 11.2 m/s 80 degrees

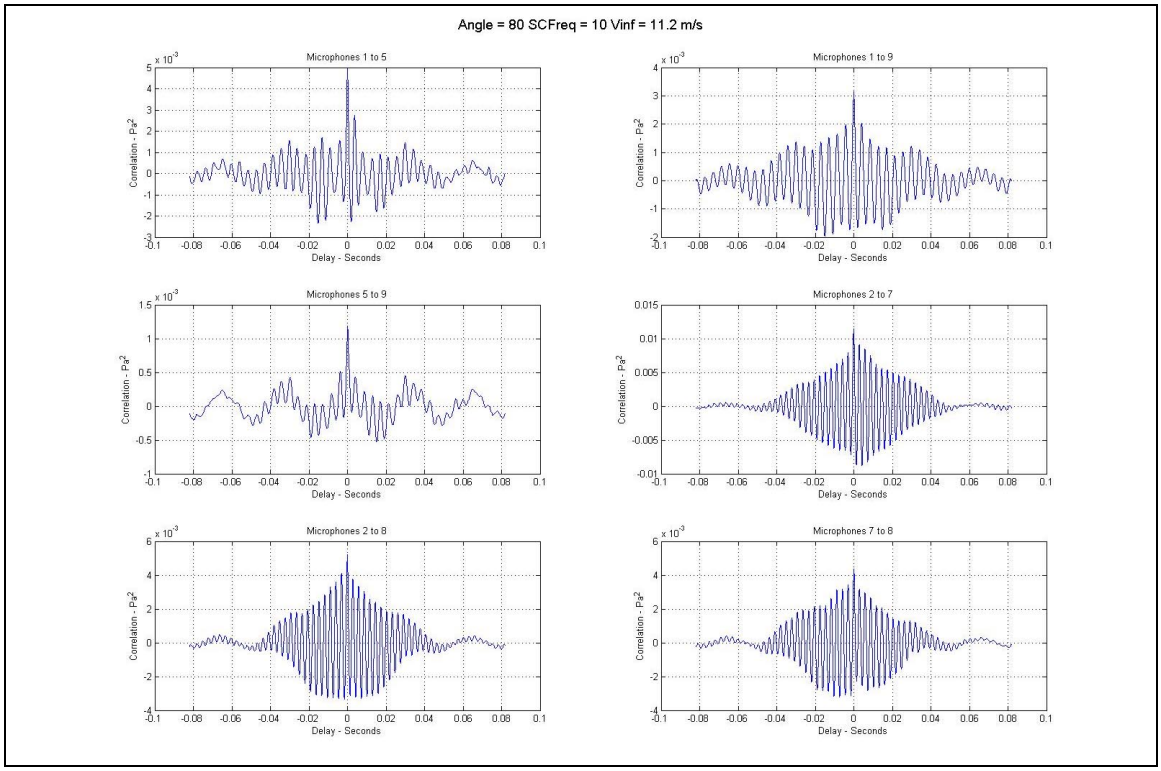

Figure 18. Cavity Cross Correlations 11.2 m/s 80 degrees

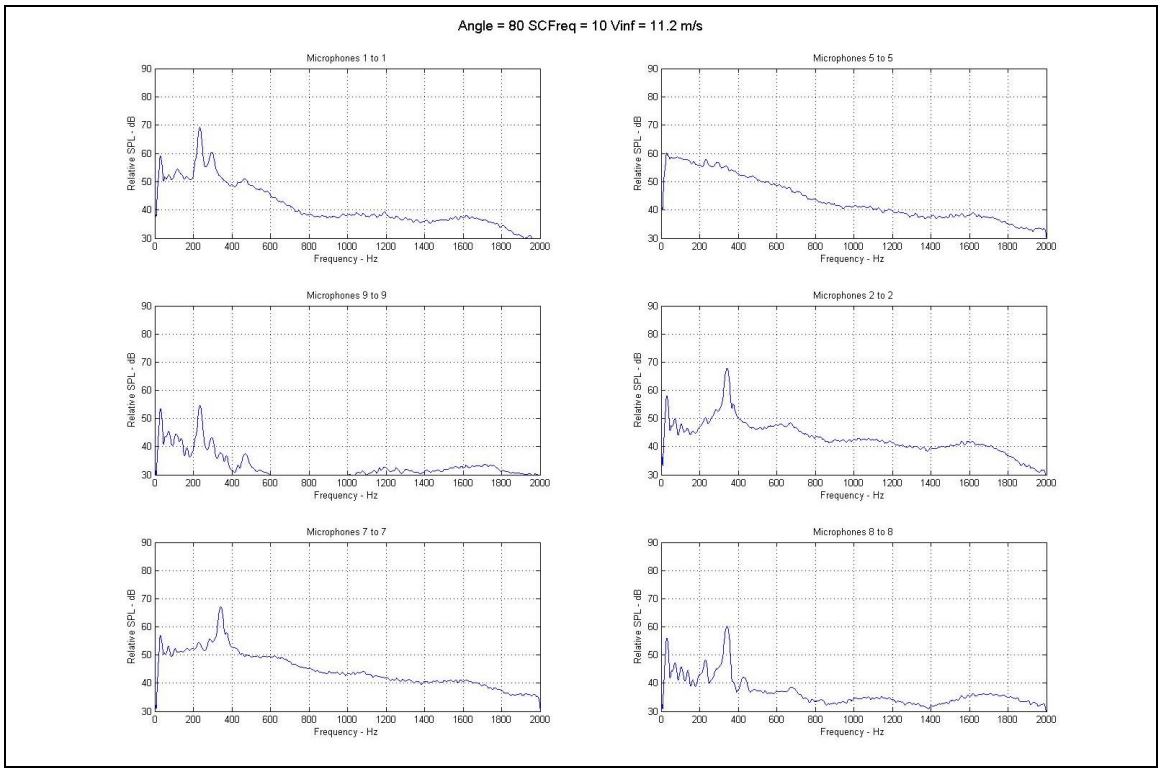

Figure 19. Cavity Auto Spectra 11.2 m/s 80 degrees

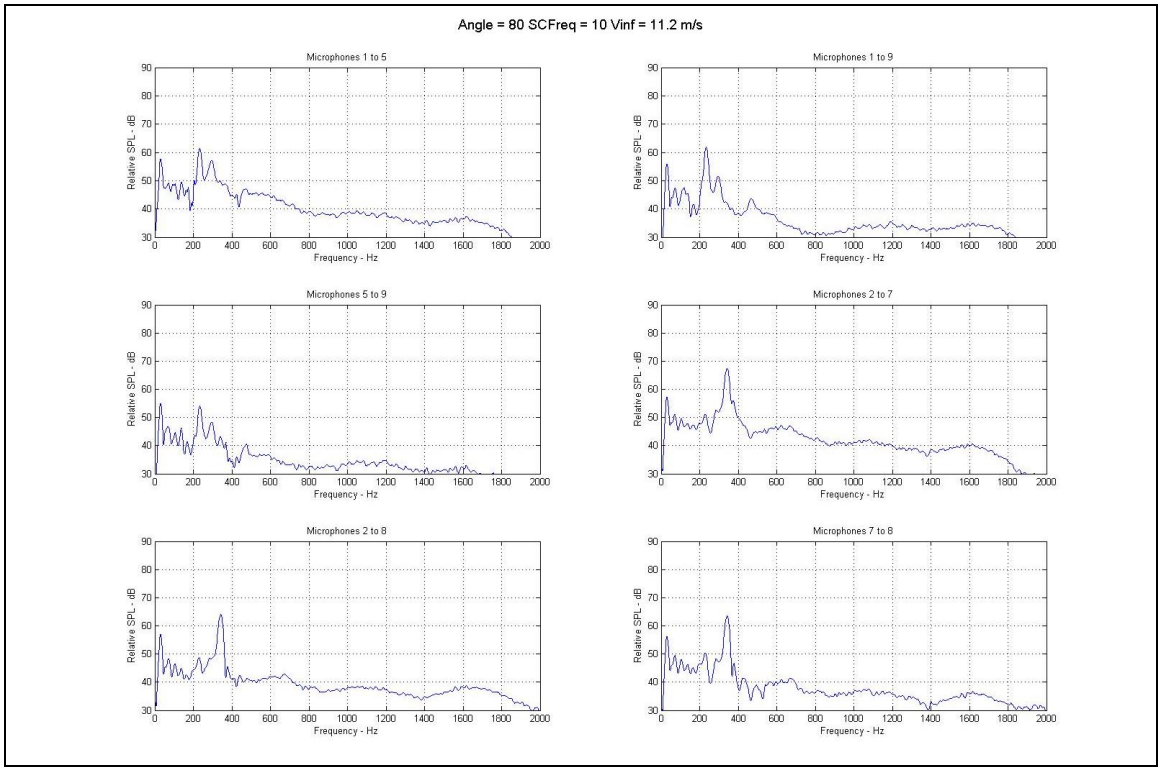

Figure 20. Cavity Cross Spectra 11.2 m/s 80 degrees

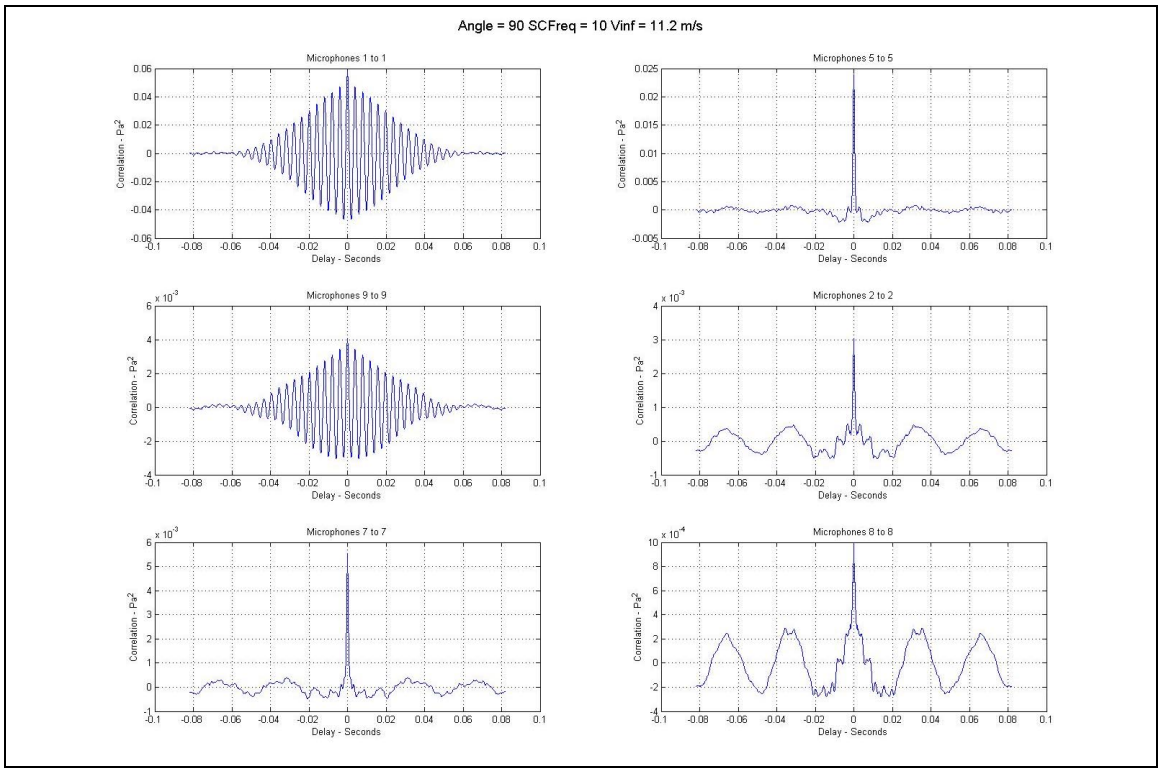

Figure 21. Cavity Auto Correlations 11.2 m/s 90 degrees

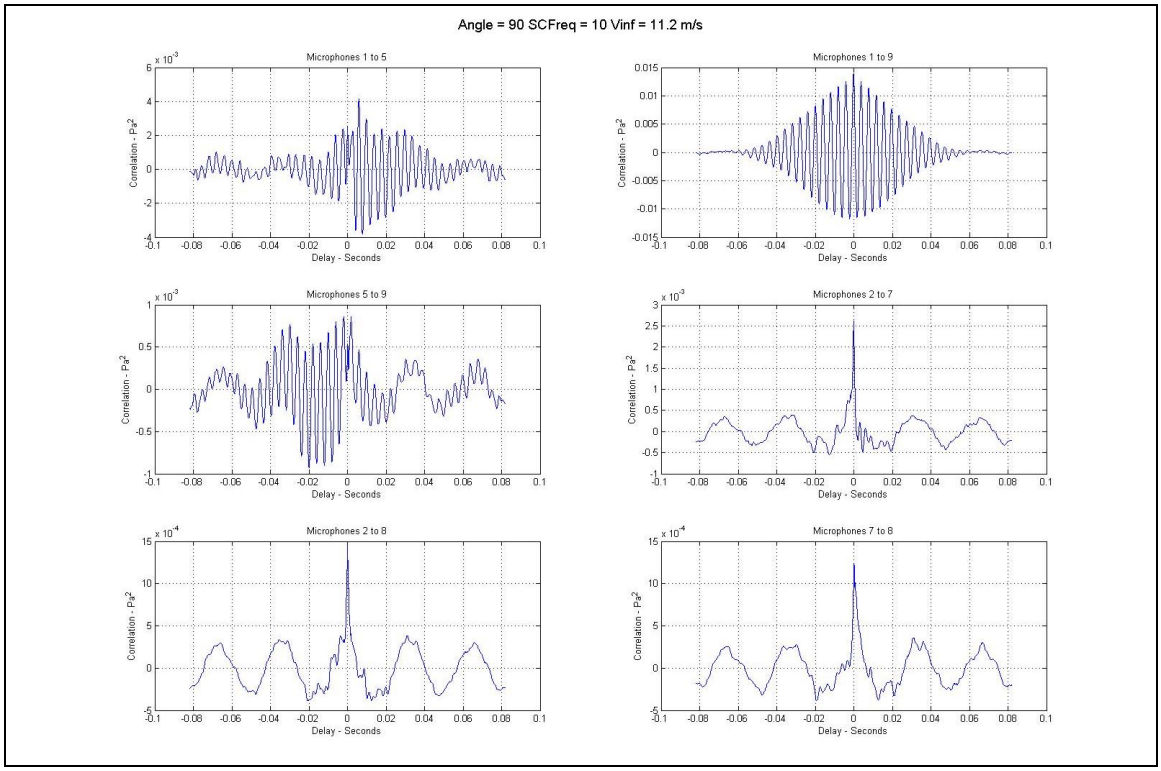

Figure 22. Cavity Cross Correlations 11.2 m/s 90 degrees

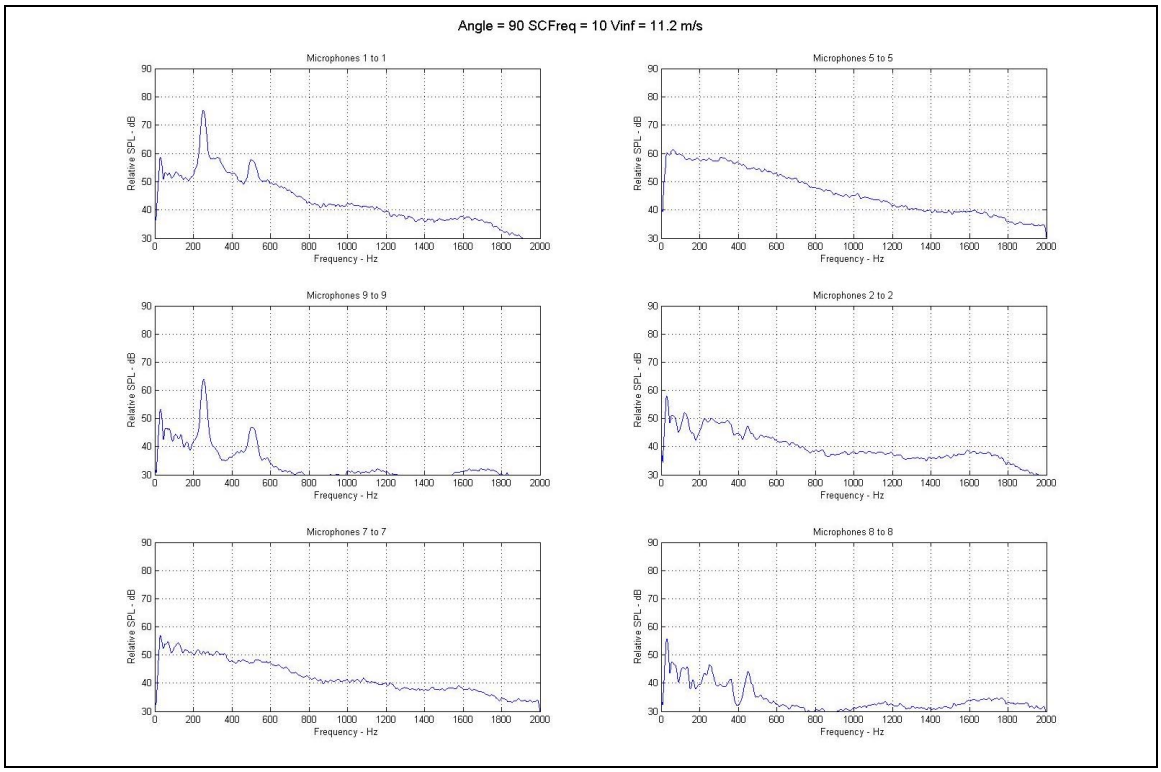

Figure 23. Cavity Auto Spectra 11.2 m/s 90 degrees

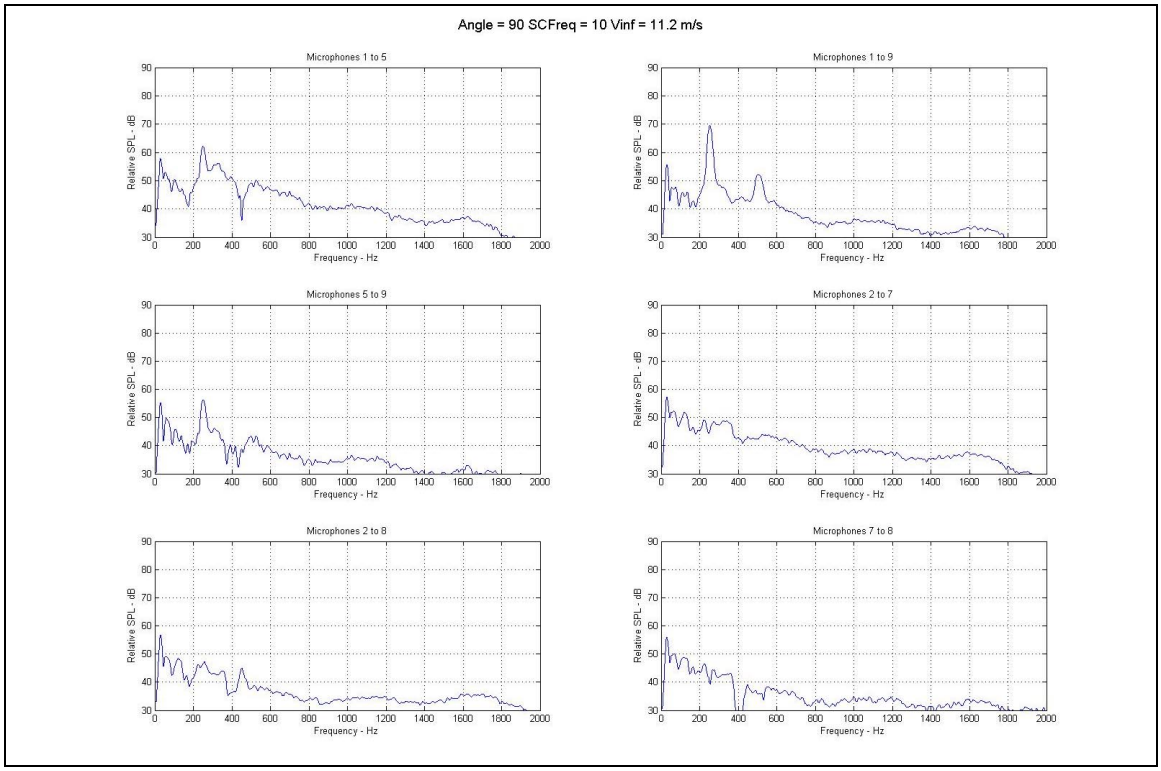

Figure 24. Cavity Cross Spectra 11.2 m/s 90 degrees

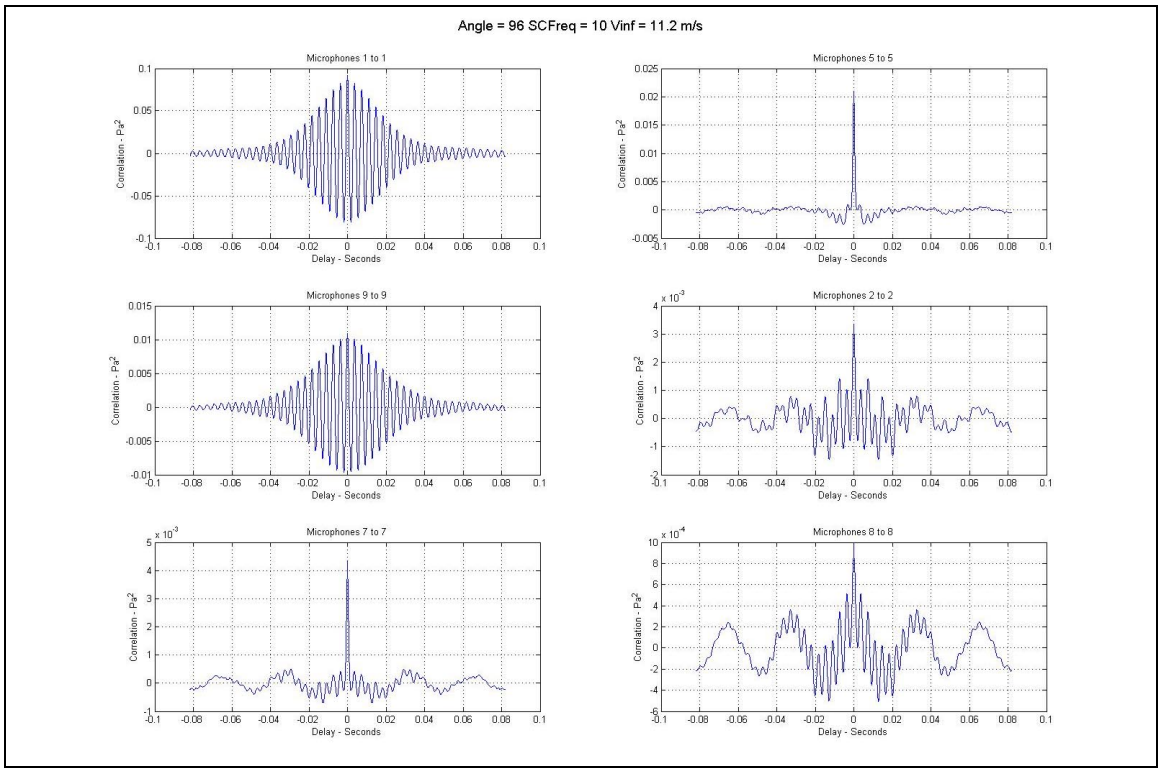

Figure 25. Cavity Auto Correlations 11.2 m/s 96 degrees

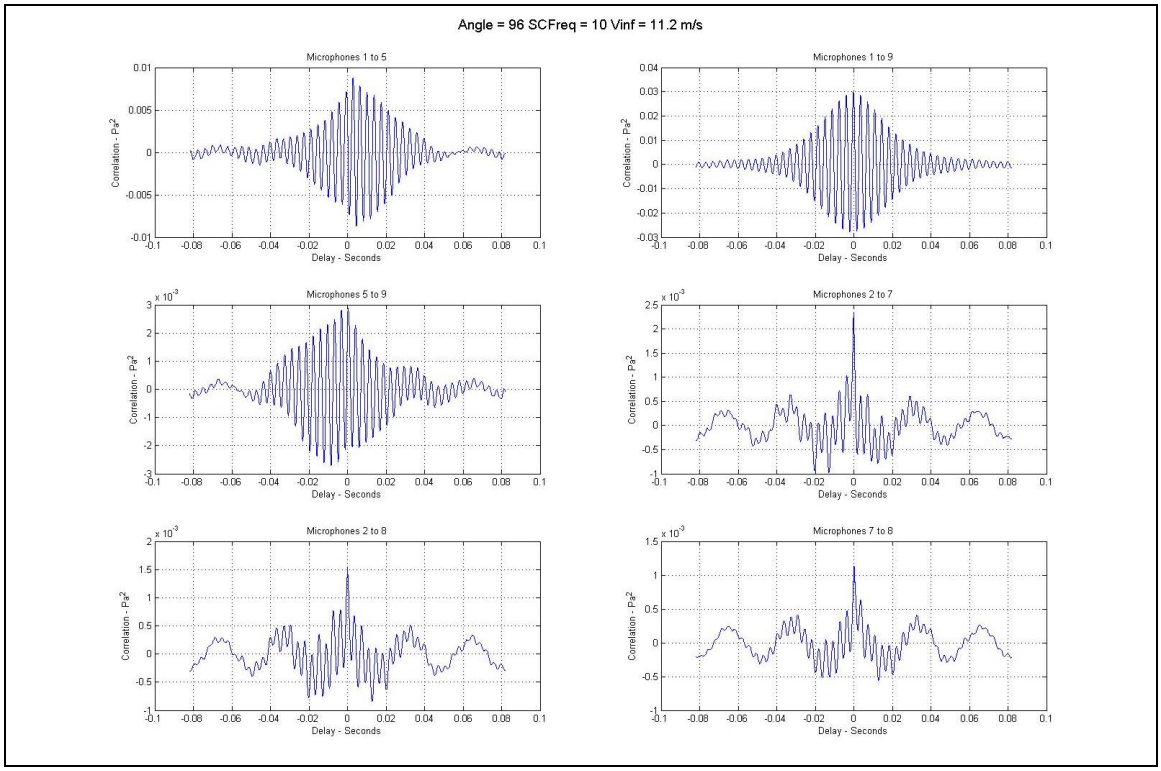

Figure 26. Cavity Cross Correlations 11.2 m/s 96 degrees

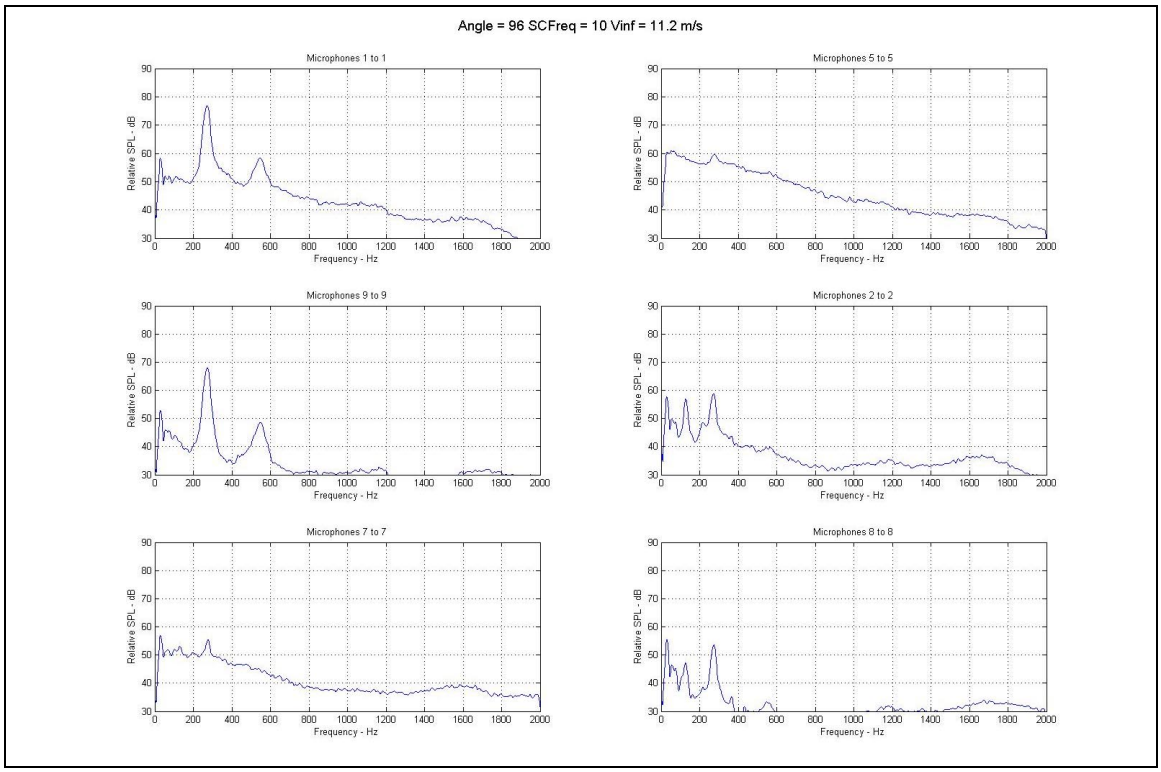

Figure 27. Cavity Auto Spectra 11.2 m/s 96 degrees

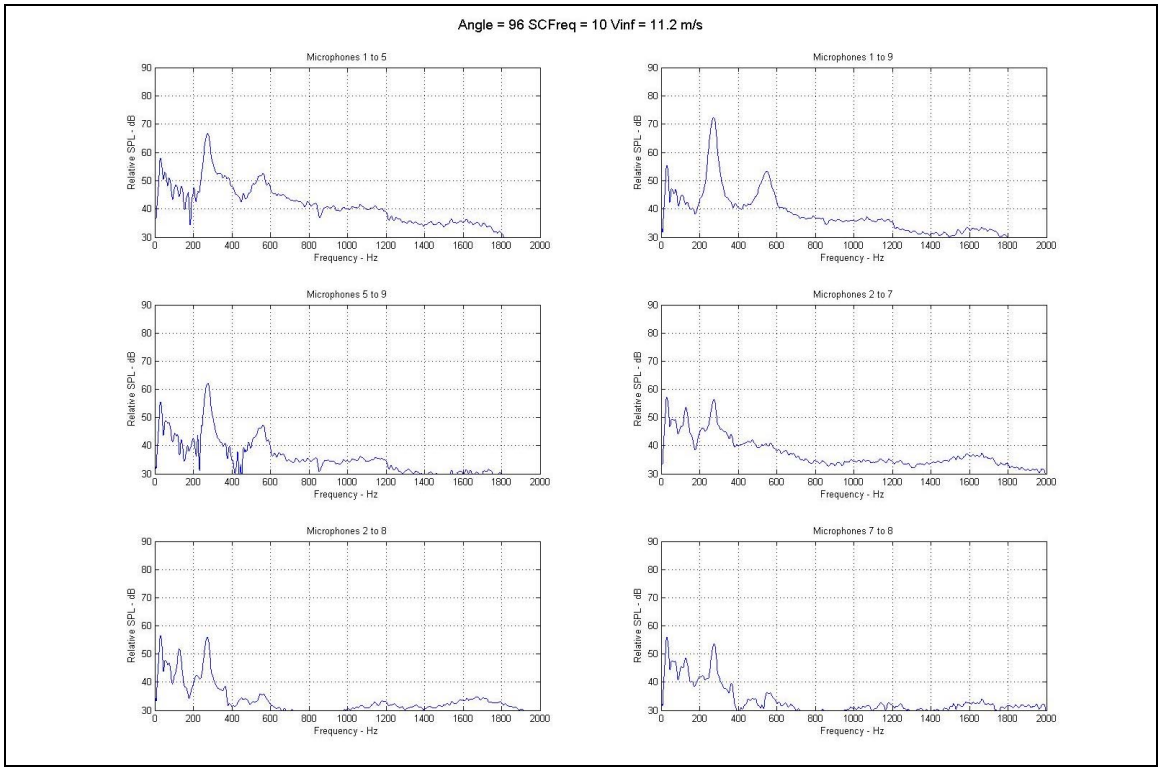

Figure 28. Cavity Cross Spectra 11.2 m/s 96 degrees

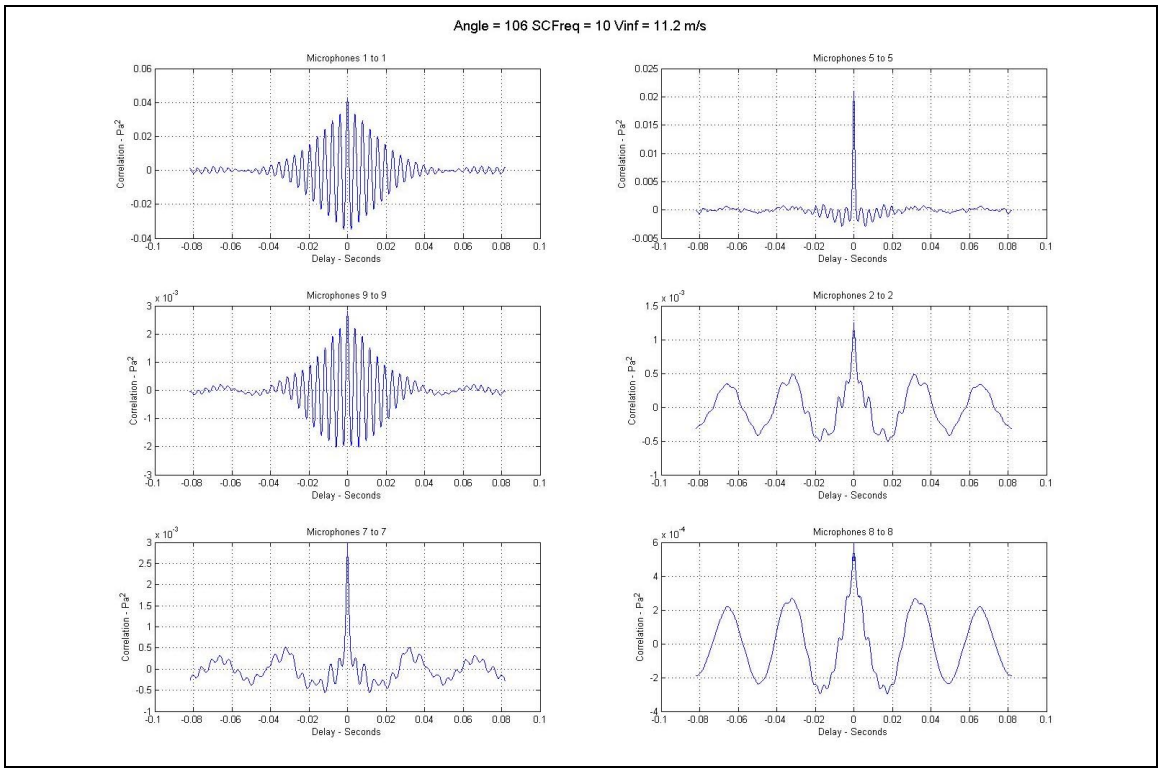

Figure 29. Cavity Auto Correlations 11.2 m/s 106 degrees

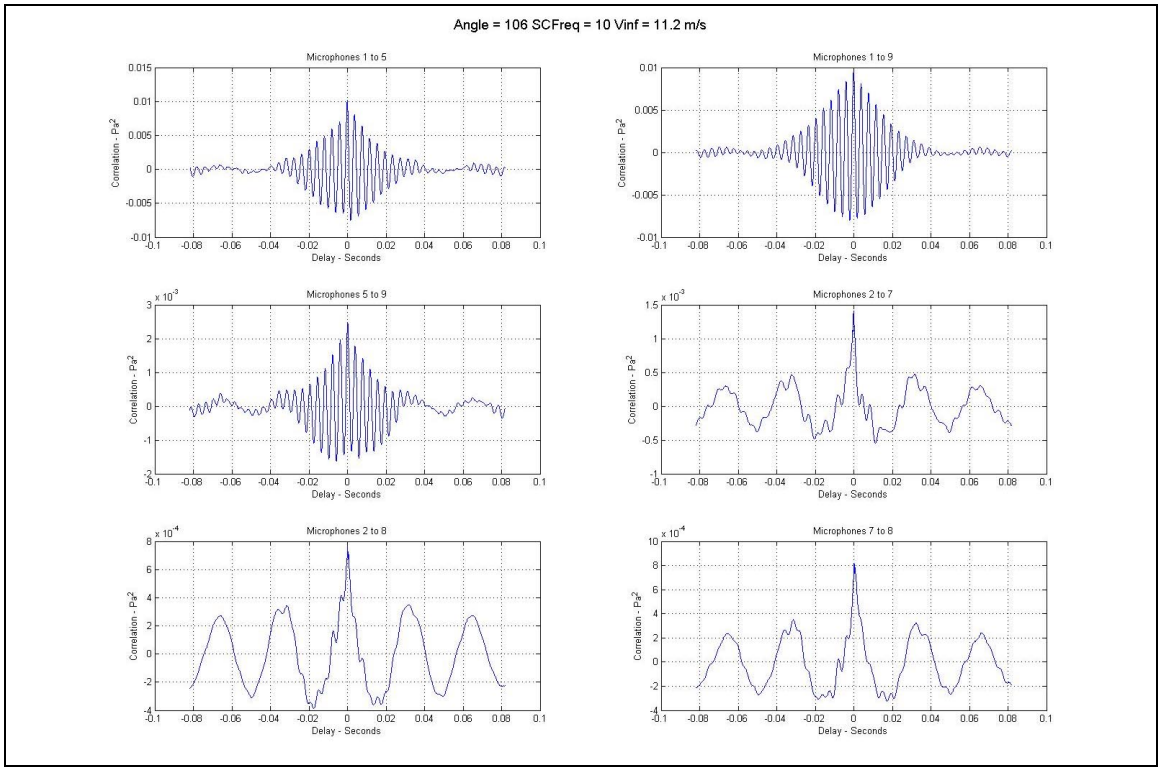

Figure 30. Cavity Cross Correlations 11.2 m/s 106 degrees

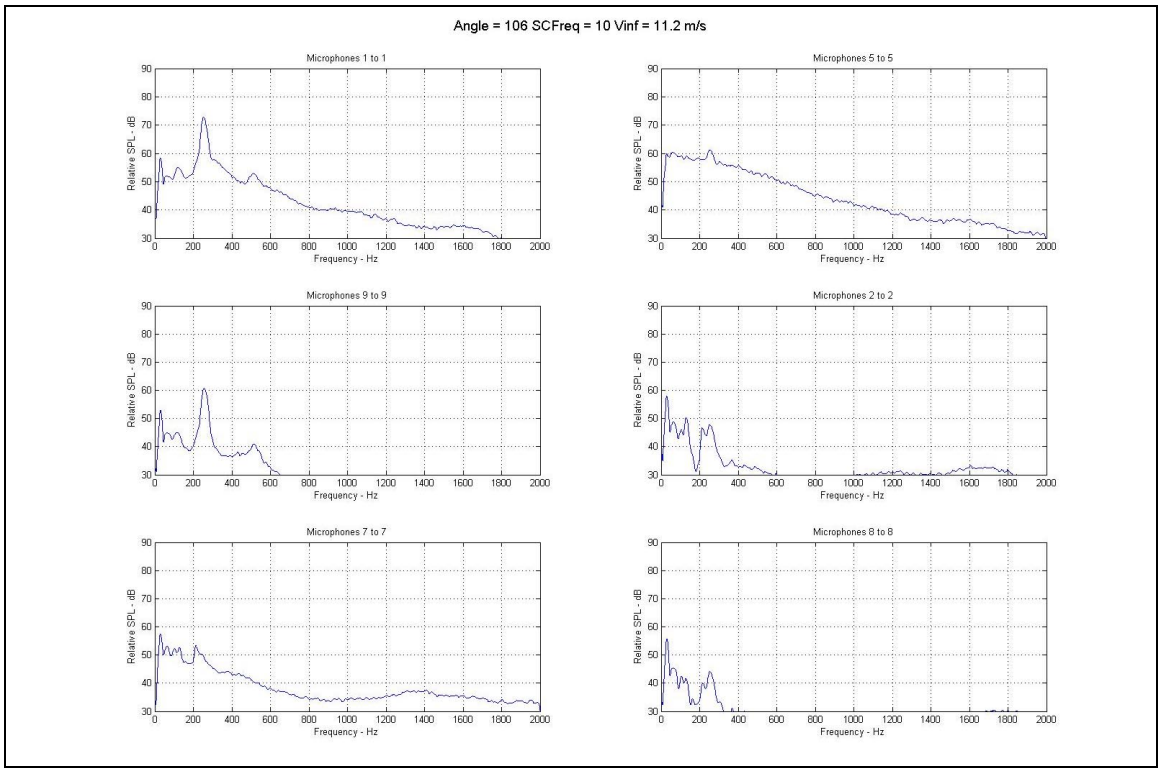

Figure 31. Cavity Auto Spectra 11.2 m/s 106 degrees

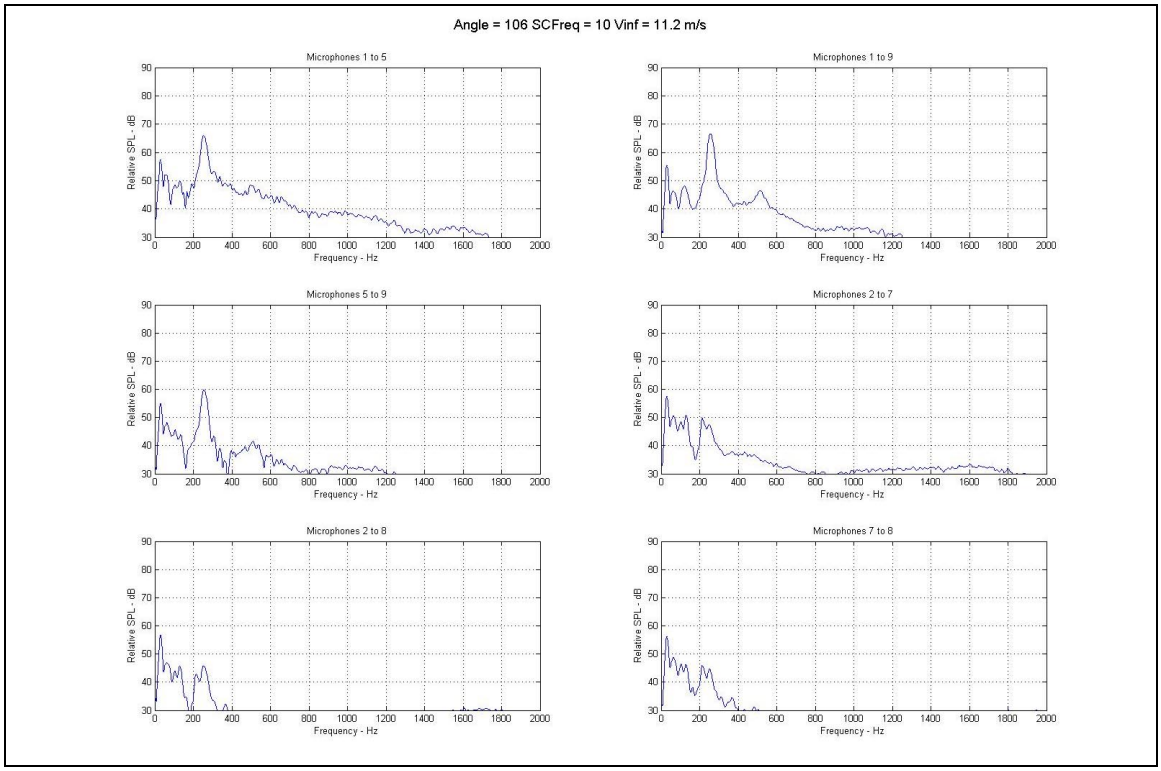

Figure 32. Cavity Cross Spectra 11.2 m/s 106 degrees

The complex response of the 2D model suggests an interaction between slots in the cascades and through-flow induced by the overhanging joint, the detailed analysis of which would be a more extensive research program. It appears, because of the phasing between face and cavity signals, that the dominant tones are representative of slot-cascade flow oscillations that could interact with duct and cavity resonances to produce high amplitude system oscillations. It was therefore decided that an investigation of the effect of changes in slot geometry on the amplitude of these flow oscillations would provide useful information relative to the potential for crack polishing or grinding to result in significant increases in overall aero-acoustic response.

Figures 33 - 36 show graphically the effects of the slot shape changes on the peak frequency and amplitude of differential tone pressure measured across the center upstream slot webbing. Note that with the exception of an apparent baseline condition anomaly at 96 and 98 degrees, the oscillation frequency is only slightly affected by the changes in the slots. However, the amplitude of the oscillation, particularly at the 7 m/s condition, is affected by up to 2 to 3 dB by the changes in slot geometry. Details of these changes, expressed as both dB and percentage pressure changes are presented in Table 3 and Table 4.

It is important to note that the absolute amplitude (approximately 80 dB) of these oscillation pressures is low, about 0.2 Pa rms, as the aeroacoustic oscillations are not supported by resonant conditions in the cavity or external flow at these frequencies. It is not necessarily the case that the same percentages changes in sound pressure observed under these conditions would translate proportionately to a resonant situation. However, the tests have demonstrated that changing the geometry of the slots in the upstream liner cascade has a modest effect on near-field aeroacoustic oscillations and that the response of the combined upstream and downstream liner cascades is dependent in a complex way on the flow speed and direction angle.

Legend for Figure 33- Figure 36:

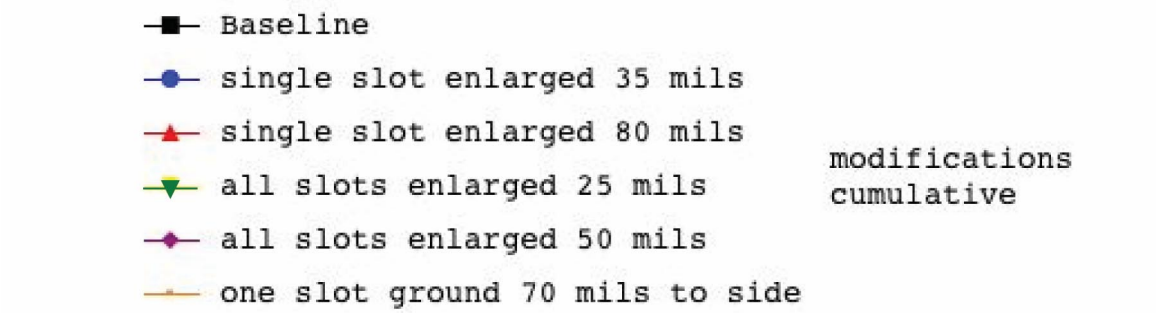

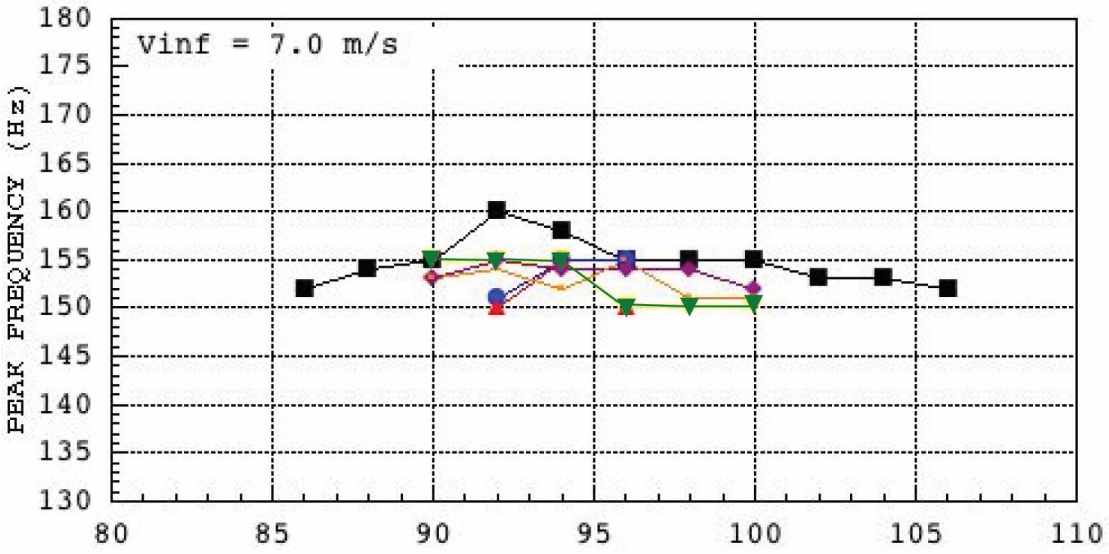

Figure 33. Frequency Variation with Upstream Slot Modification Configurations at 7 m/s

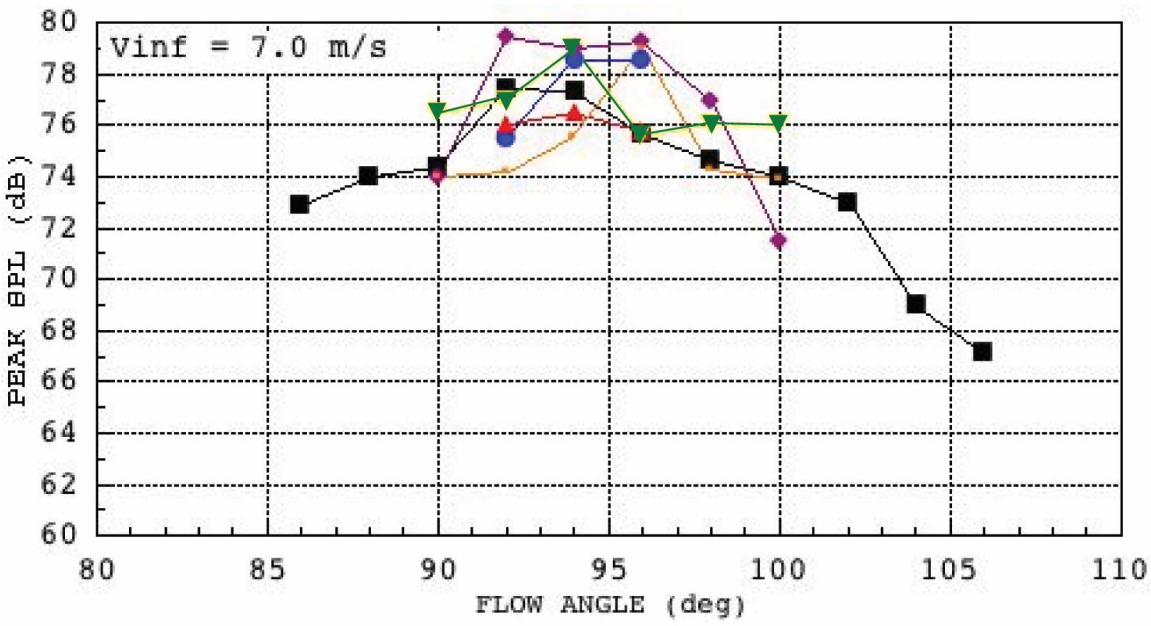

Figure 34. Amplitude Variation with Upstream Slot Modification Configurations at 7 m/s

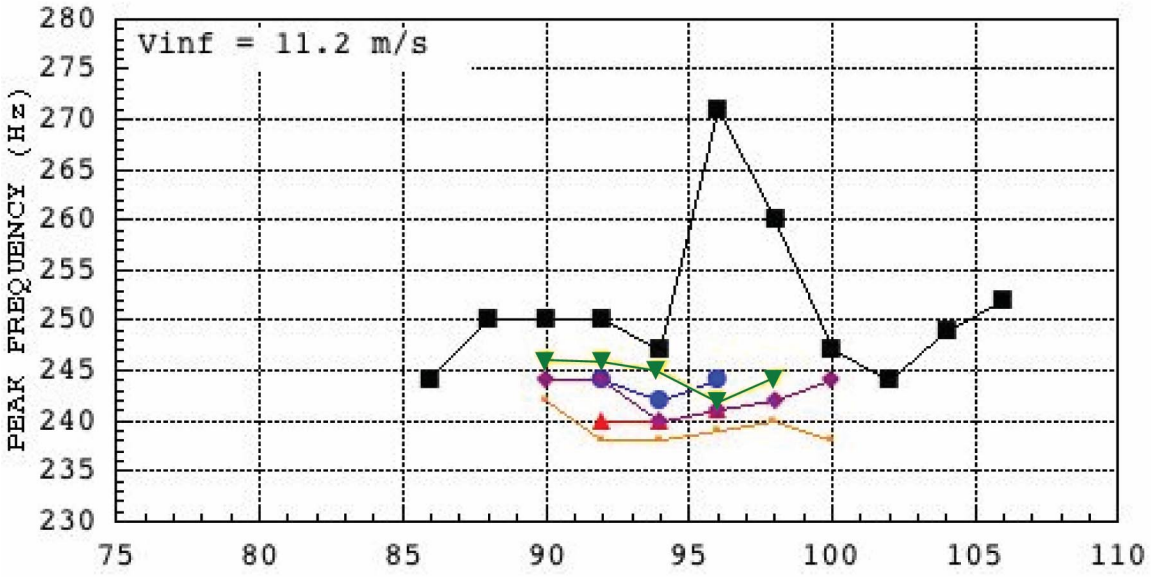

Figure 35. Frequency Variation with Upstream Slot Modification Configurations at 11.2 m/s

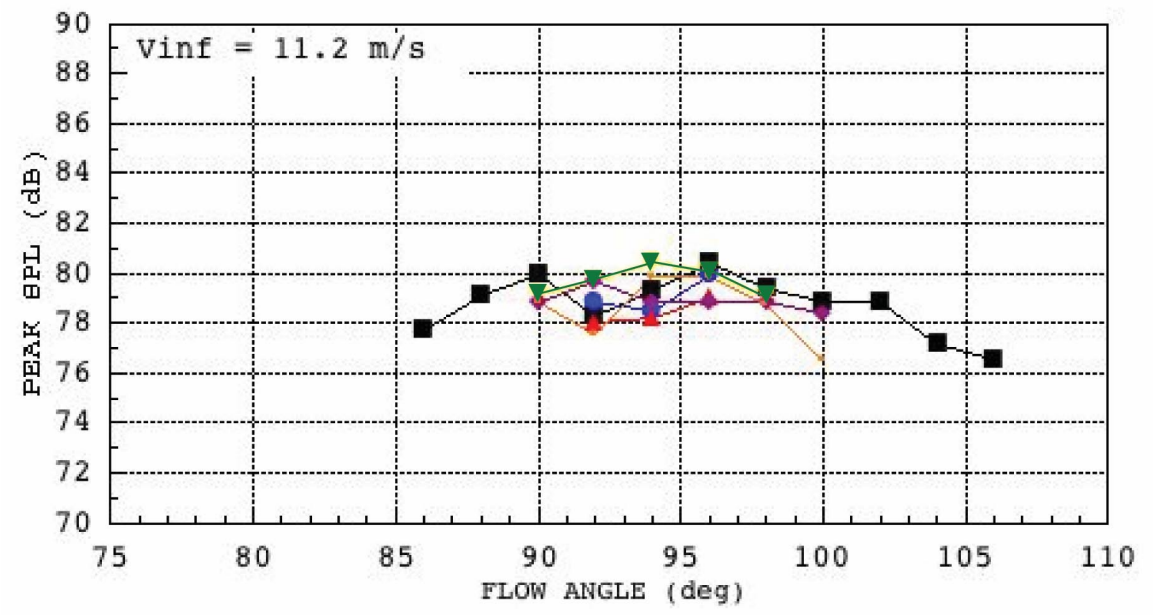

Figure 36. Amplitude Variation with Upstream Slot Modification Configurations at 11.2 m/s

Table 3. Changes in SPL and Percent Change in Pressure Differential vs Angle at 7 m/s

7.0 m/s	Upstream Slot Changes in Peak Tone Amplitude									
Angle	single slot enlarged 35 mils		single slot enlarged 80 mils		all slots enlarged 25 mils		all slots enlarged 50 mils		one slot ground 70 mils to side	
deg	dB	Pct	dB	Pct	dB	Pct	dB	Pct	dB	Pct
90					2.1	27.4	-0.4	-4.5	-0.4	-4.5
92	-1.9	-19.6	-1.4	-14.9	-0.4	-4.5	2.1	27.4	-3.2	-30.8
94	1.2	14.8	-0.8	-8.8	1.7	21.6	1.7	21.6	-1.7	-17.8
96	2.8	38.0	0.1	1.2	-0.1	-1.1	3.6	51.4	3.3	46.2
98					1.4	17.5	2.4	31.8	-0.3	-3.4
100					2	25.9	-2.5	-25.0	-0.1	-1.1

Table 4. Changes in SPL and Percent Change in Pressure Differential vs Angle at 11.2 m/s

11.2 m/s	Upstream Slot Changes in Peak Tone Amplitude									
Angle	single slot enlarged 35 mils		single slot enlarged 80 mils		all slots enlarged 25 mils		all slots enlarged 50 mils		one slot ground 70 mils to side	
deg	dB	Pct	dB	Pct	dB	Pct	dB	Pct	dB	Pct
90					-0.9	-9.8	-1.1	-11.9	-1.1	-11.9
92	0.6	7.2	-0.3	-3.4	1.4	17.5	1.4	17.5	-0.7	-7.7
94	-0.8	-8.8	-1.1	-11.9	1.1	13.5	-0.4	-4.5	0.6	7.2
96	-0.4	-4.5	-1.4	-14.9	-0.3	-3.4	-1.5	-15.9	-0.5	-5.6
98					-0.4	-4.5	-0.5	-5.6	-0.6	-6.7
100							-0.5	-5.6	-2.4	-24.1

A more detailed illustration of the 96-98 degree peak frequency anomaly is presented in Figures 37 - 38. Note the baseline spectral peak is significantly broader than that of the modified slot peak and that for the modified slot case, a secondary spectral peak has "appeared" at about 300 Hz. On close examination, it can be seen that in the baseline condition, the two peaks are merged, resulting in a slightly increased sound level and skewed peak shape with increased peak frequency. Modifying the slots (Condition C shown) caused the secondary peak frequency to migrate upward and eliminate its influence on the observed frequency and amplitude of the main peak.

A potential ramification of this latter observation is that if slots in the cascade are rendered dissimilar by crack polishing, peak frequencies associated with slot edge tone may become spread out and less likely to become synchronized with duct modes, resulting overall in a reduced probably of high amplitude oscillations in the flowliner.

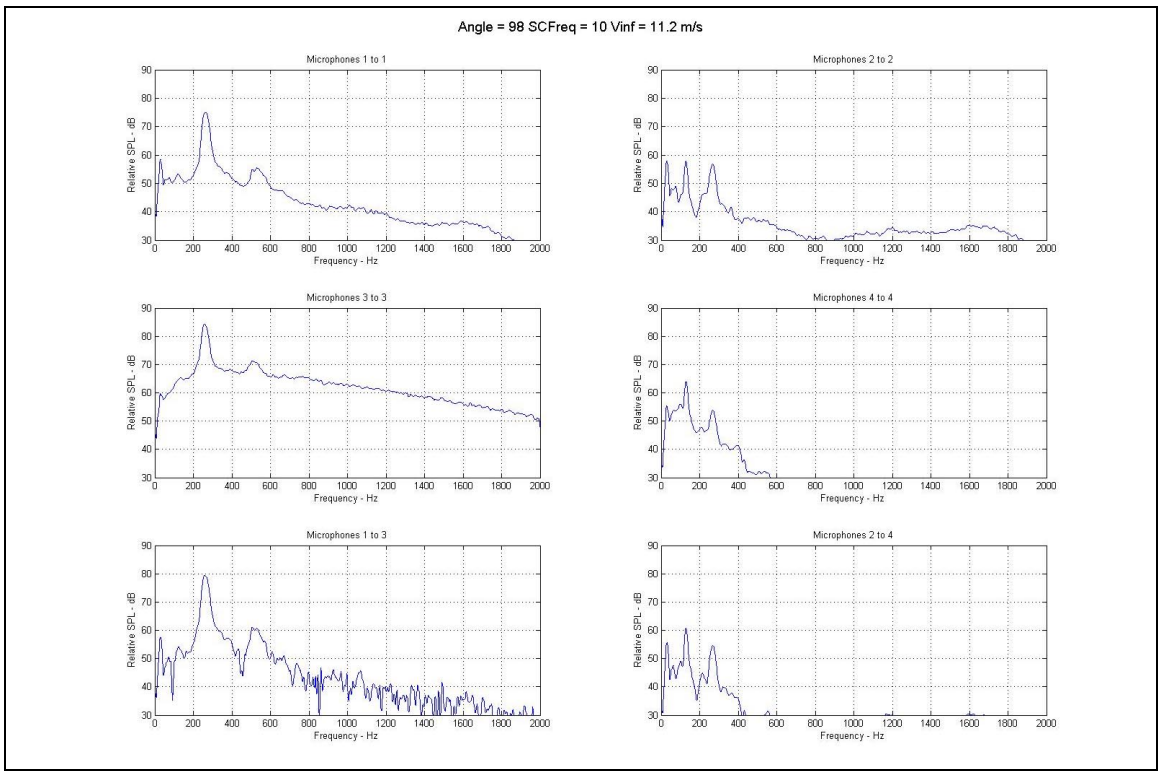

Figure 37. Spectral Details for 11.2 m/s 96 deg – Baseline (wide peak centered at 270 Hz)

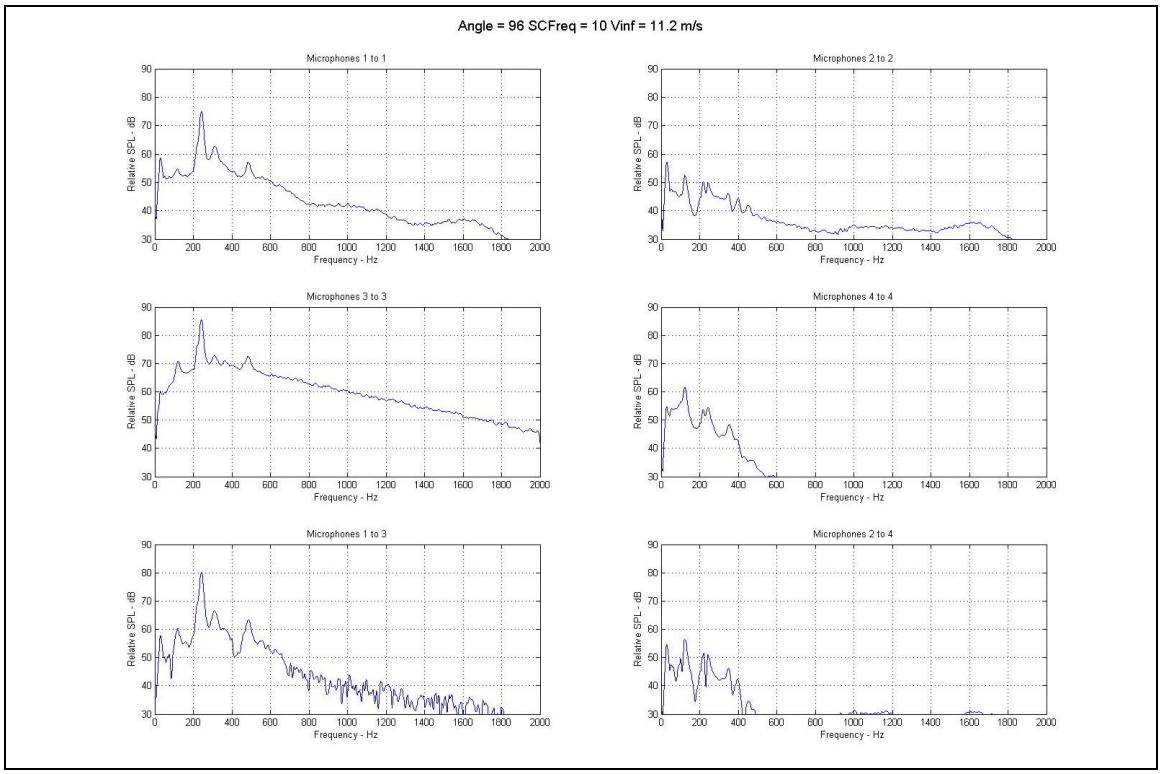

Figure 38. Spectral Details for 11.2 m/s 96 deg – Slot Condition C (narrow peaks at 240 and 310 Hz)

Higher Flow Speed Tests

Following completion of these tests, it was found that small cracks in the downstream liner may be more prevalent that previously observed, and results of 3D airflow testing by Boeing/Rocketdyne indicated that at higher swirling velocities, high amplitude "edge tones" were observed both with upstream slots open and taped. The reported speed range corresponds to the 30-40 m/s range shown in Figure 3, in which a downstream-dominant tone was observed at $Nst \approx 0.3$ (1700 Hz at 37 m/s).

A brief investigation of this issue was conducted by collecting test data under the following conditions:

- Wind Tunnel velocity 31 and 37.6 m/s
- Incidence Angle 90° and 105°
- Three Slot Conditions
    - All open, upstream machined to Condition G
    - Upstream slots taped closed
    - Downstream slots taped closed

The results of the 90° incidence tests are presented in Figures 39 - 44, which show relative cross-spectral amplitudes and phases between upstream and downstream webbing faces and liner cavities. Peak spectral sound levels were identified and are summarized in Table 5.

The following observations are offered:

Slots Open

Up to approximately 80 Hz, low frequency tunnel noise is dominant and in phase in both liner segments.

At approx. 80 Hz at 31 m/s and 110 Hz at 37.6 m/s, broadband noise begins a phase rotation in the downstream liner

At 1500 Hz for 31 m/s and 1700 Hz for 37.6 m/s, a pronounced spectral peak occurs in both upstream and downstream liners, with face to cavity phase approximately 50-60°.

Upstream Slots Taped

100-200 Hz broadband noise increase 5 dB with phase reversal at upstream liner

Approximately 5 dB reduction of 1500-1700 Hz peak at upstream liner

Approximately 2 dB reduction of 1500-1700 Hz peak at downstream liner

Downstream Slots Taped

100-160 Hz broadband noise increase 5-7 dB at downstream liner

Reduction of 1500-1700 Hz peak to broadband level (at least -16 dB) at downstream liner.

It is clear from these results that the downstream liner slots are the dominant source mechanism for the 1700 Hz range spectral peak. Some insight on why this occurs is revealed by face-to-cavity transfer functions presented in Figures 45 - 48 and 50. Note the linear gain scale.

At low 11.2 m/s with all slots open, corresponding to the majority of slot modification testing, upstream cavity response peaks with 180° phase in the 250-350 Hz range is noted, followed by a smaller rise in the 500-700 Hz (second harmonic?) range with 0° phase. In the downstream cavity, strong gain is observed near 1700 Hz, although the actual amplitude is small compared to the overall noise as seen in Figures 49 and 51

At higher 37.6 m/s the downstream peak at 1700 Hz is sharpened as the cavity response begins to reinforce slot cascade shedding. Although the response is too weak to induce high amplitude oscillation, it is still of sufficient amplitude to be seen above the boundary layer noise in Figure 52.

Table 5. Summary of High Swirl Flow Test Results

Upstream Cavity SPL				
Speed – m/s	31		37.6	
Peak Frequency - Hz	1490		1650	
Angle - deg	90	105	90	105
Baseline Preliminary	75	NA	82	NA
Slots Open (Cond. G)	70	70	80	78
Upstream Slots Taped	71	70	76	73
Downstream Slots Taped	68	63	72	70
Downstream Cavity SPL				
Baseline Preliminary	80	NA	88	NA
Slots Open (Cond. G)	73	73	82	80
Upstream Slots Taped	76	74	80	77
Downstream Slots Taped	63	60	69	66

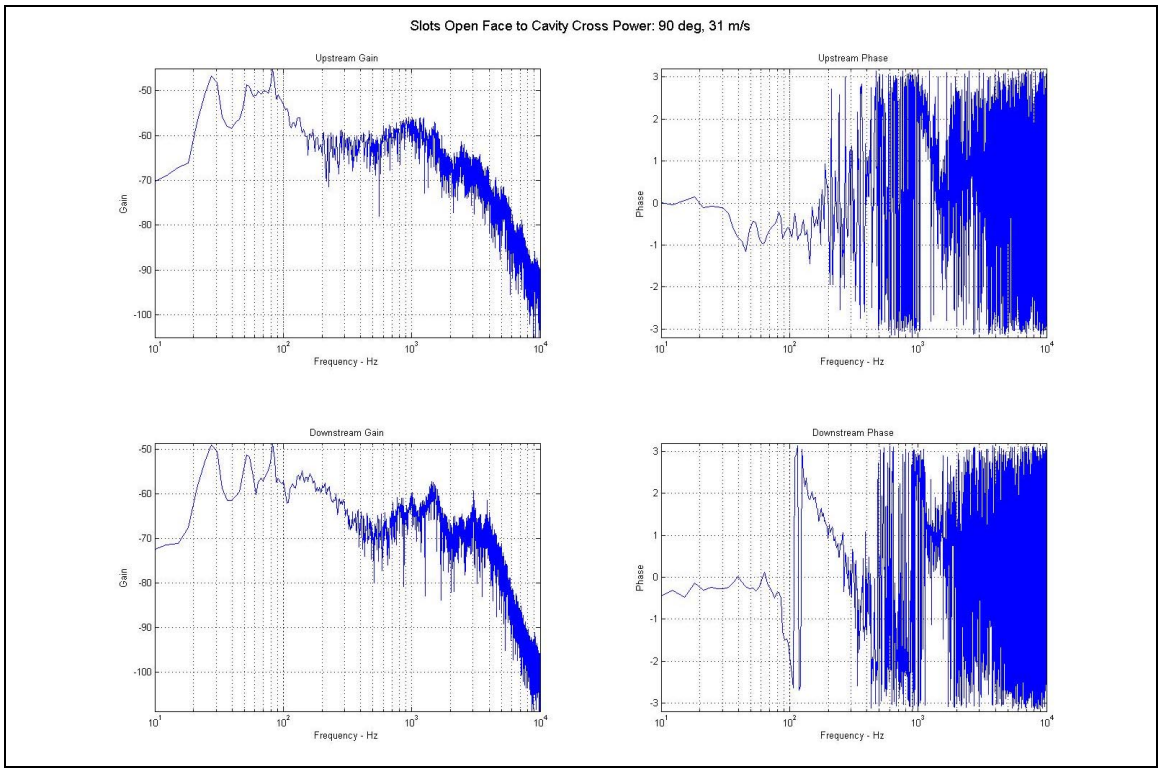

Figure 39. Face to Cavity Cross Power Spectra and Phase for Slots Open, 31 m/s at 90 deg

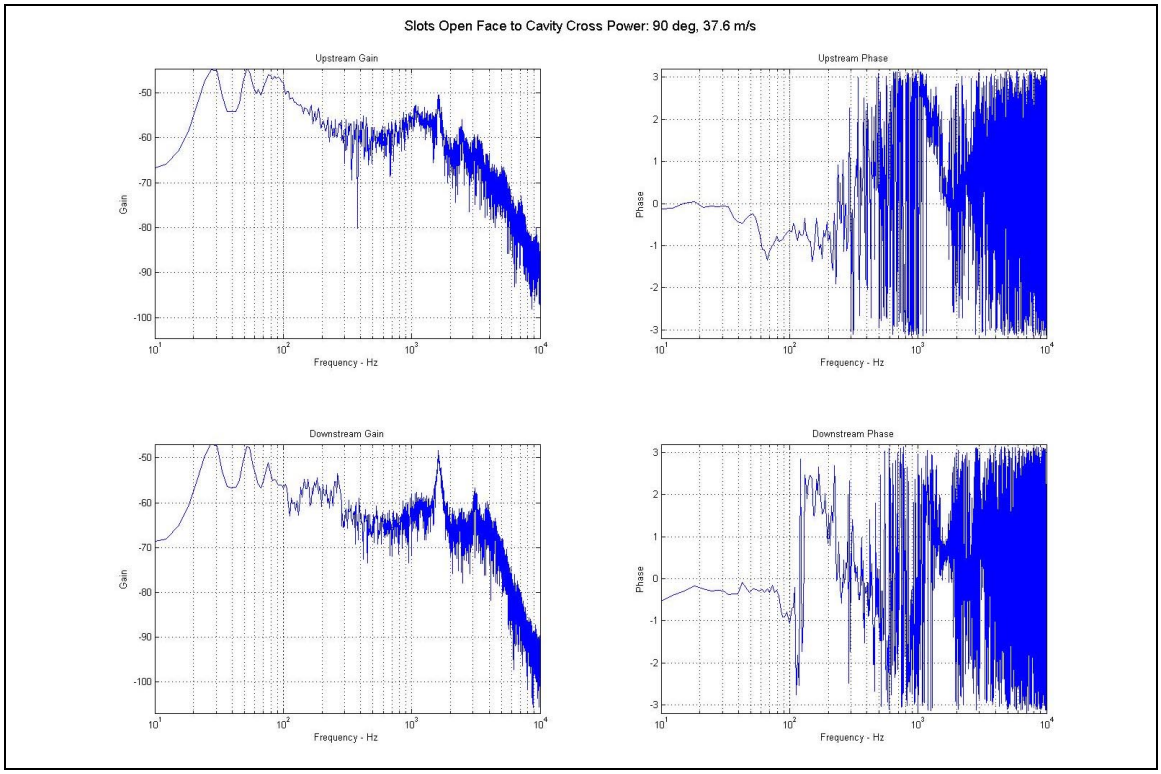

Figure 40. Face to Cavity Cross Power Spectra and Phase for Slots Open, 37.6 m/s at 90 deg

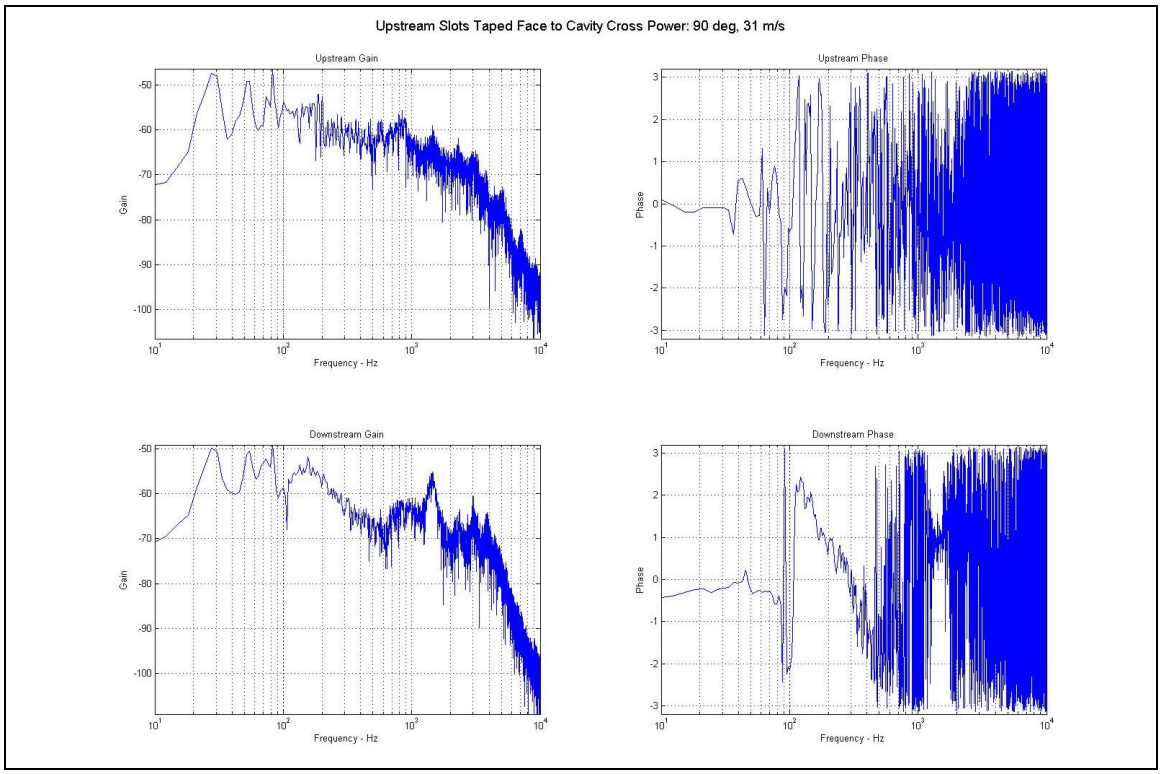

Figure 41. Face to Cavity Cross Power Spectra with Upstream Slots Taped, 31 m/s 90 deg

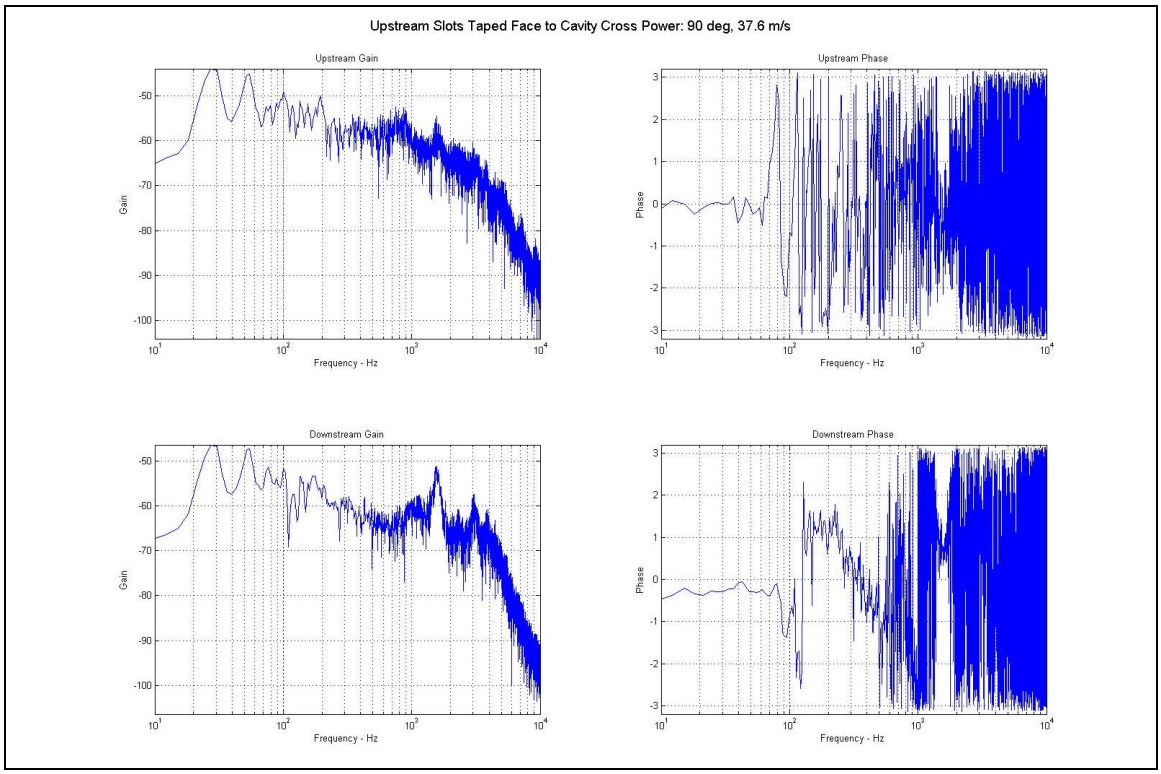

Figure 42. Face to Cavity Cross Power Spectra with Upstream Slots Taped, 37.6 m/s 90 deg

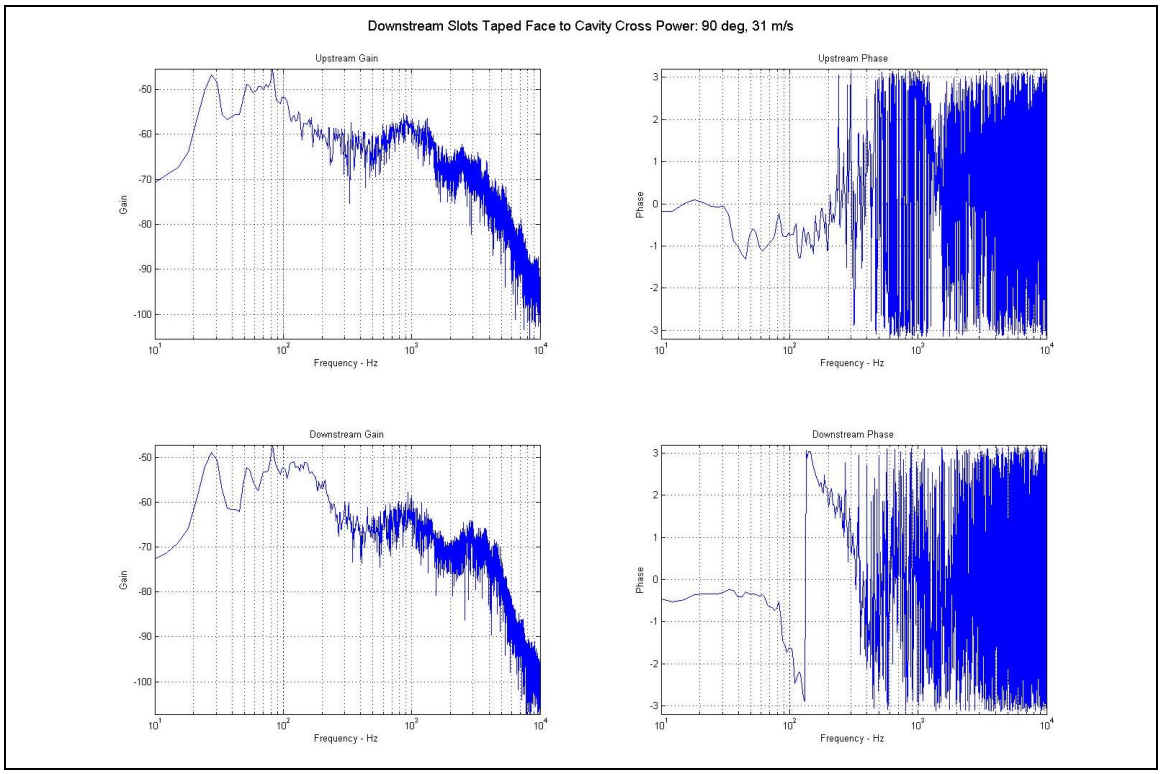

Figure 43. Face to Cavity Cross Power Spectra with Downstream Slots Taped, 31 m/s 90 deg

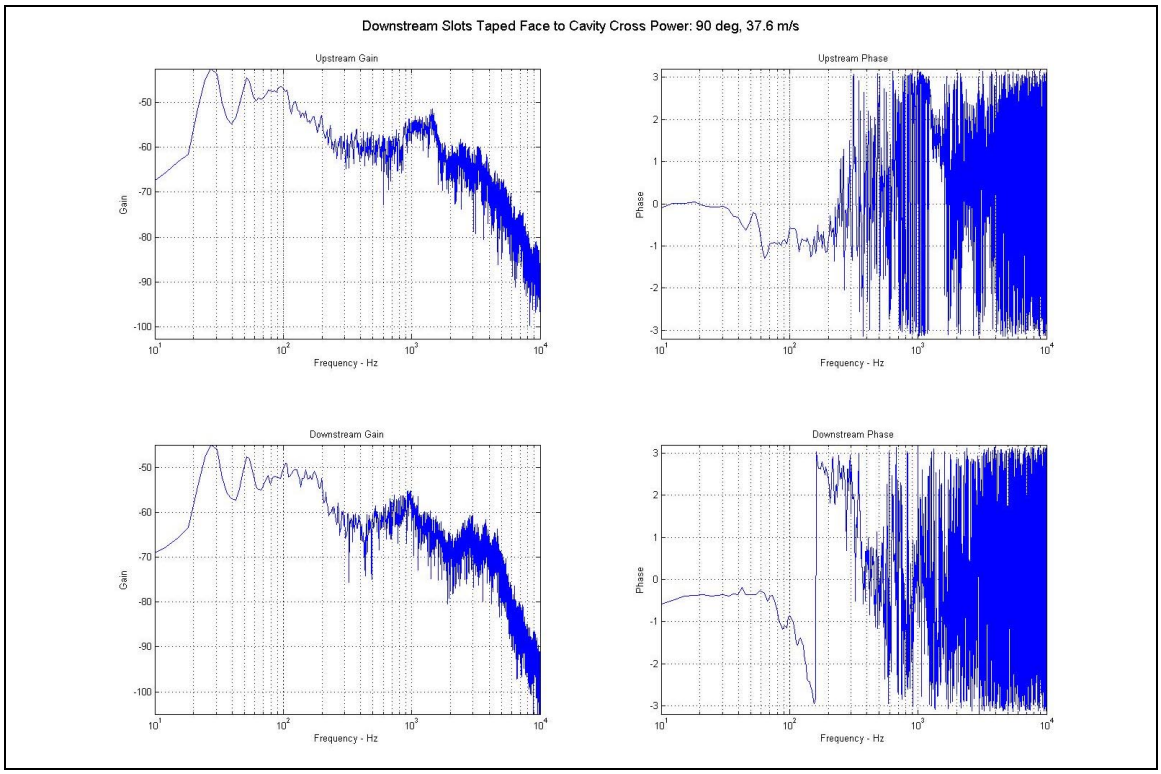

Figure 44. Face to Cavity Cross Power Spectra with Downstream Slots Taped, 37.6 m/s 90 deg

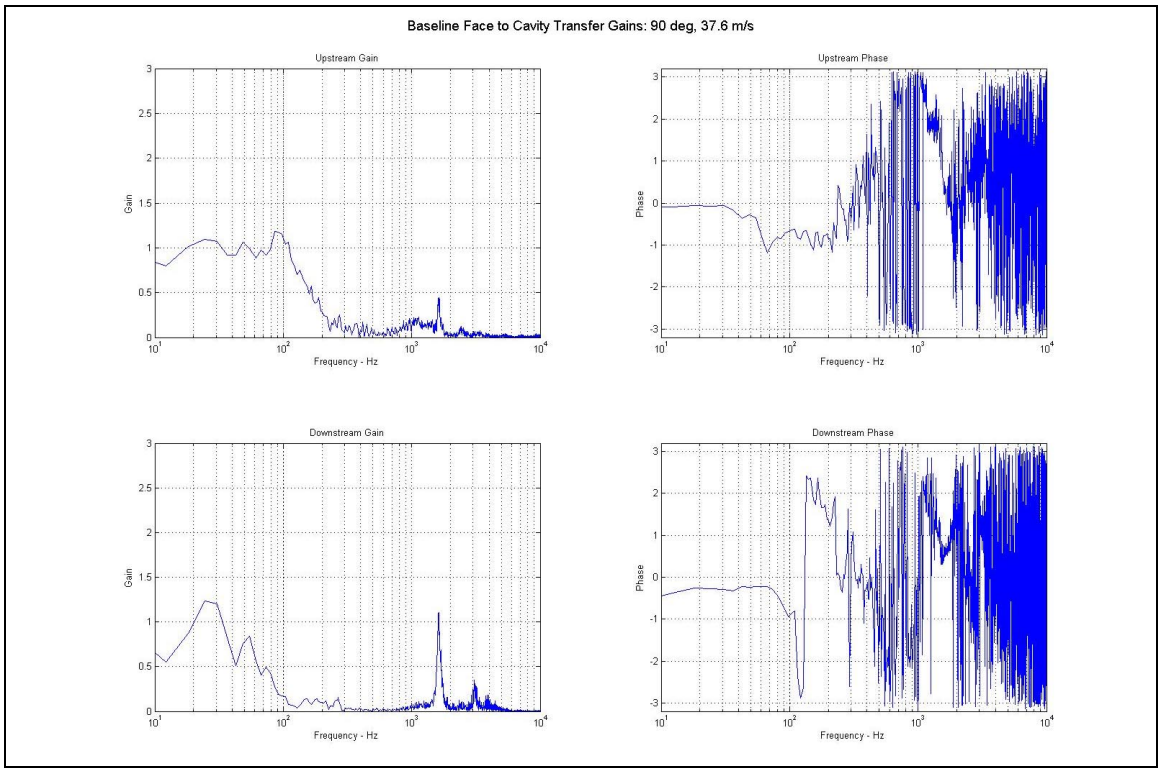

Figure 45. Face to Cavity Transfer Functions Slots Open, 37.6 m/s 90 deg

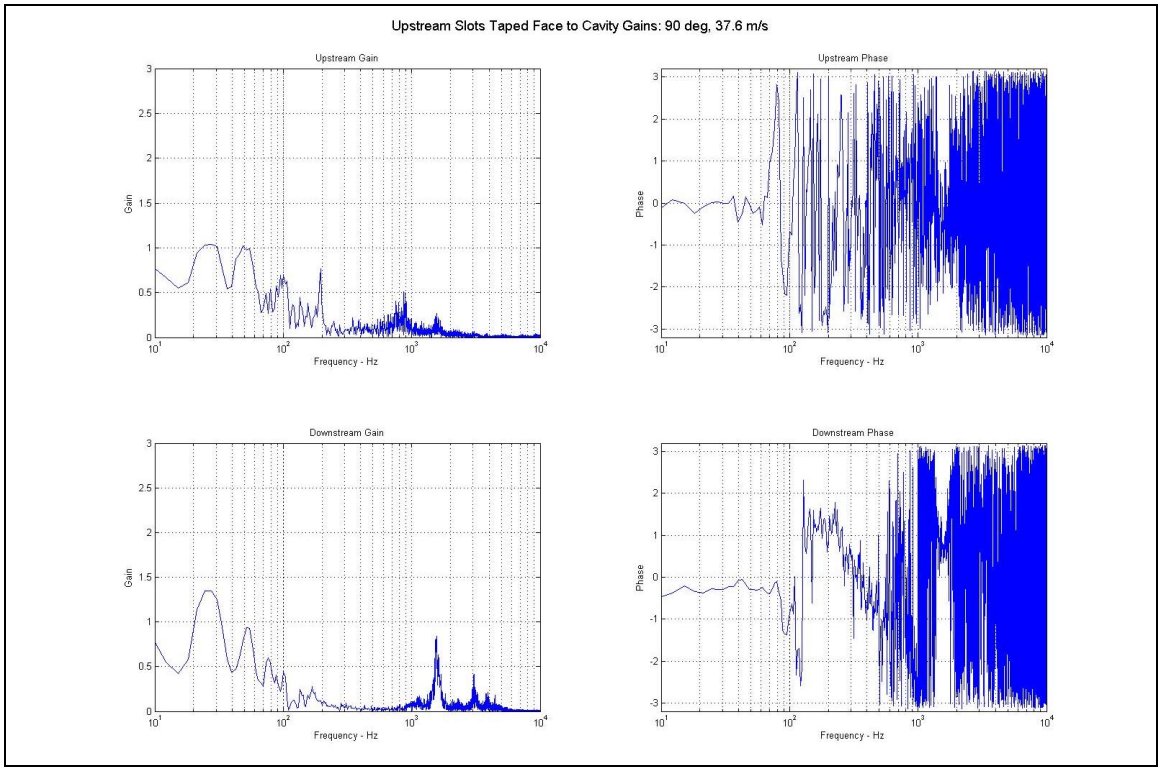

Figure 46. Face to Cavity Transfer Functions Upstream Slots Taped, 37.6 m/s 90 deg

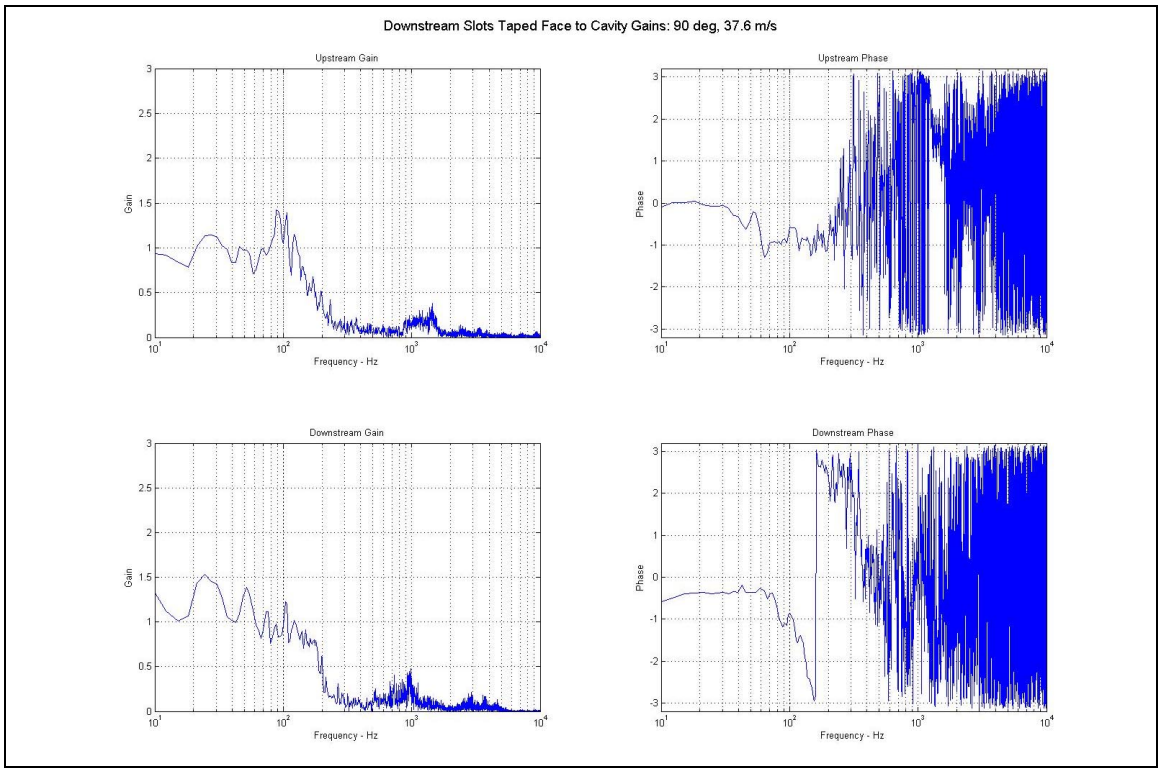

Figure 47. Face to Cavity Transfer Functions Downstream Slots Taped, 37.6 m/s 90 deg

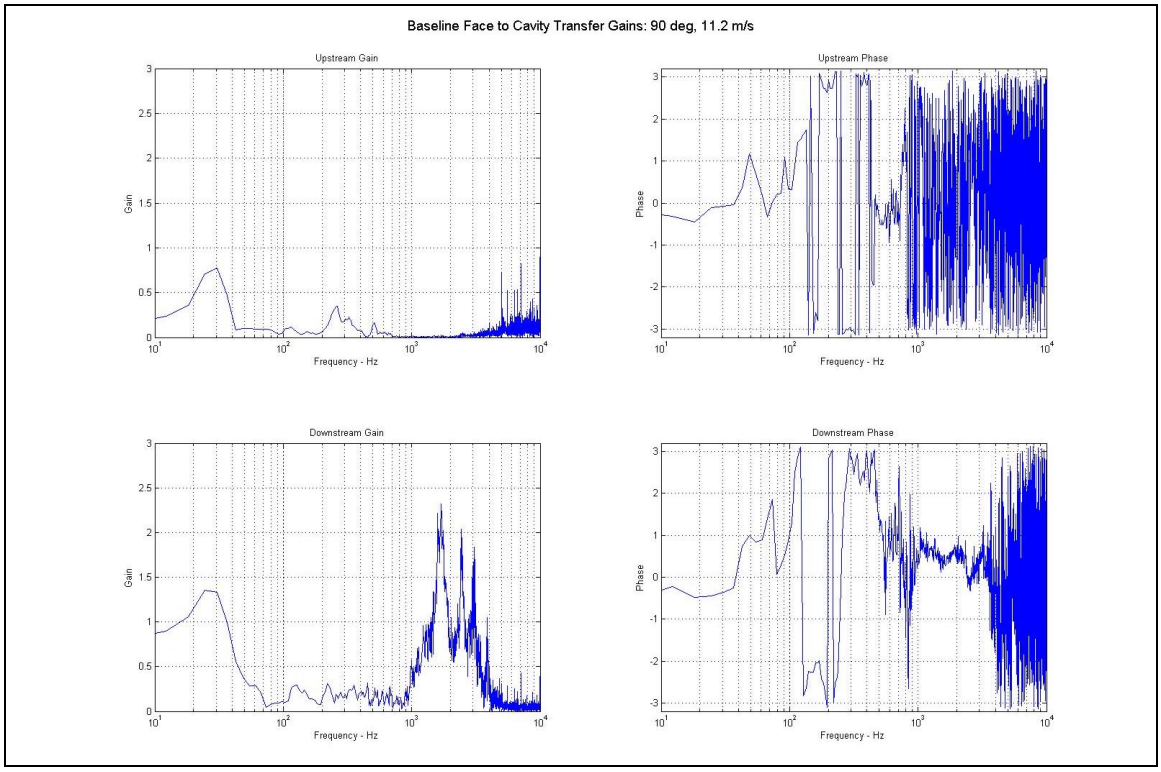

Figure 48. Face to Cavity Transfer Functions Slots Open, 11 m/s 90 deg

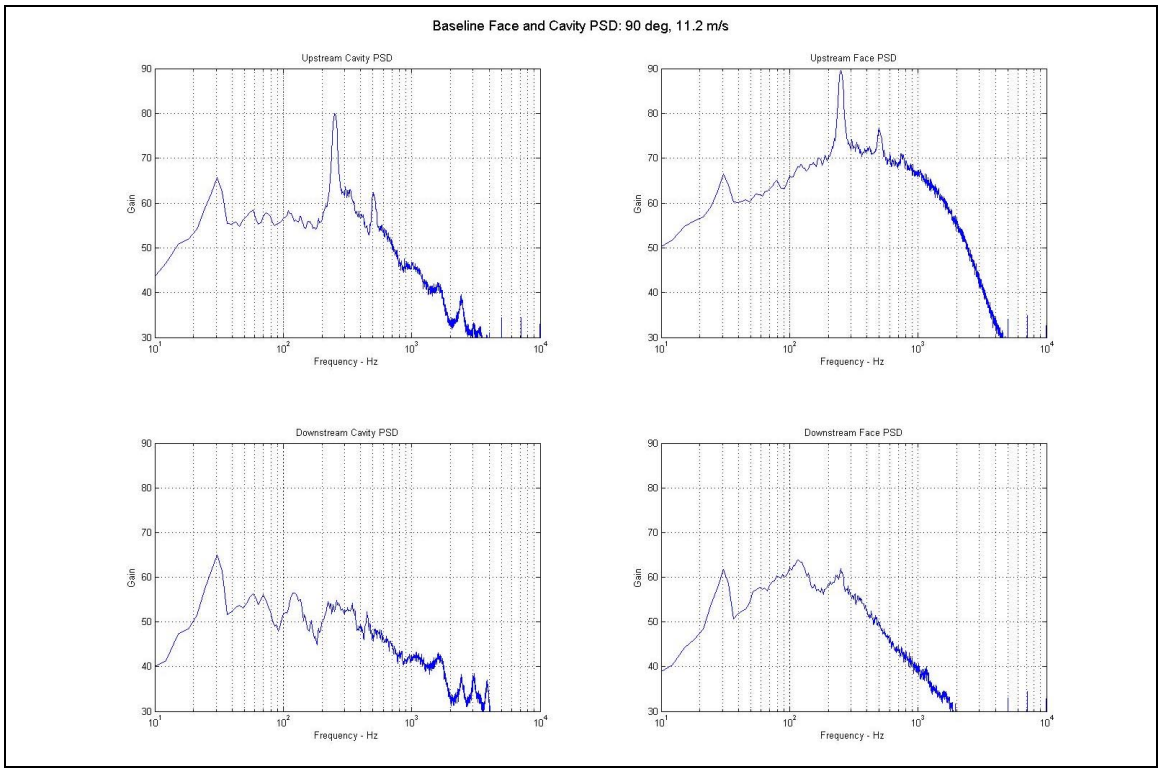

Figure 49. Face and Cavity Spectra, Slots Open, 11 m/s 90 deg

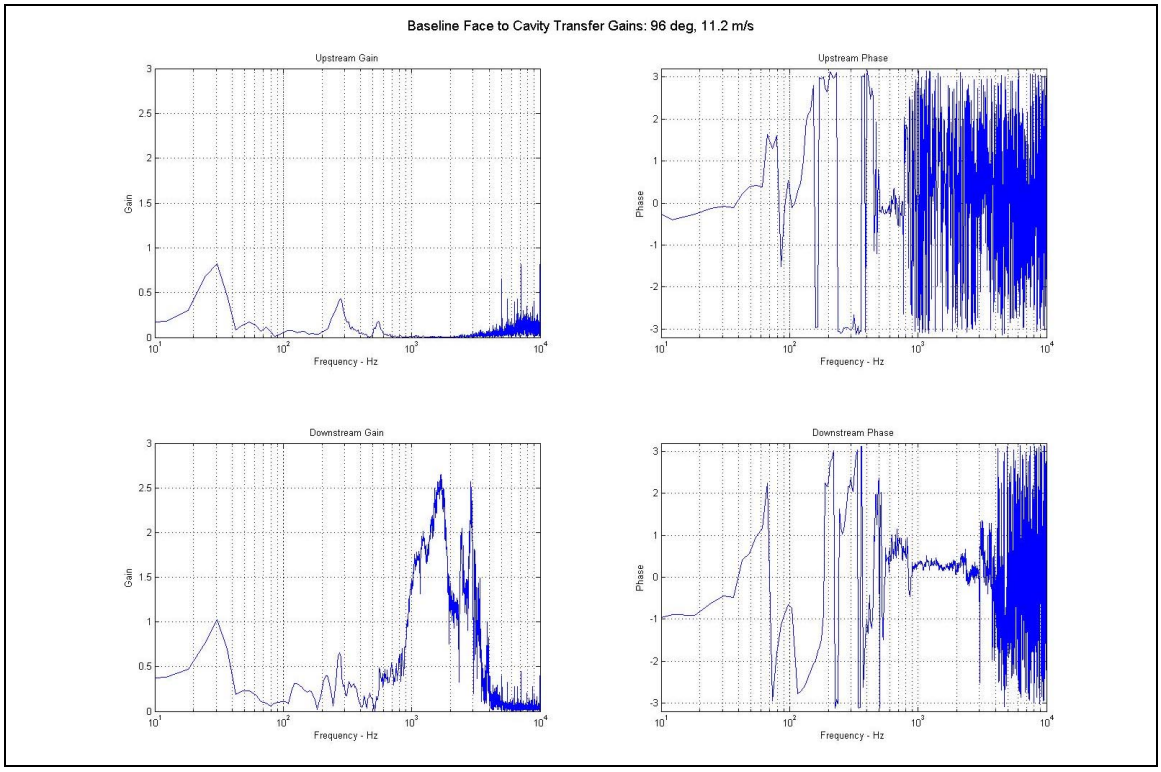

Figure 50. Face to Cavity Transfer Functions Slots Open, 11 m/s 96 deg

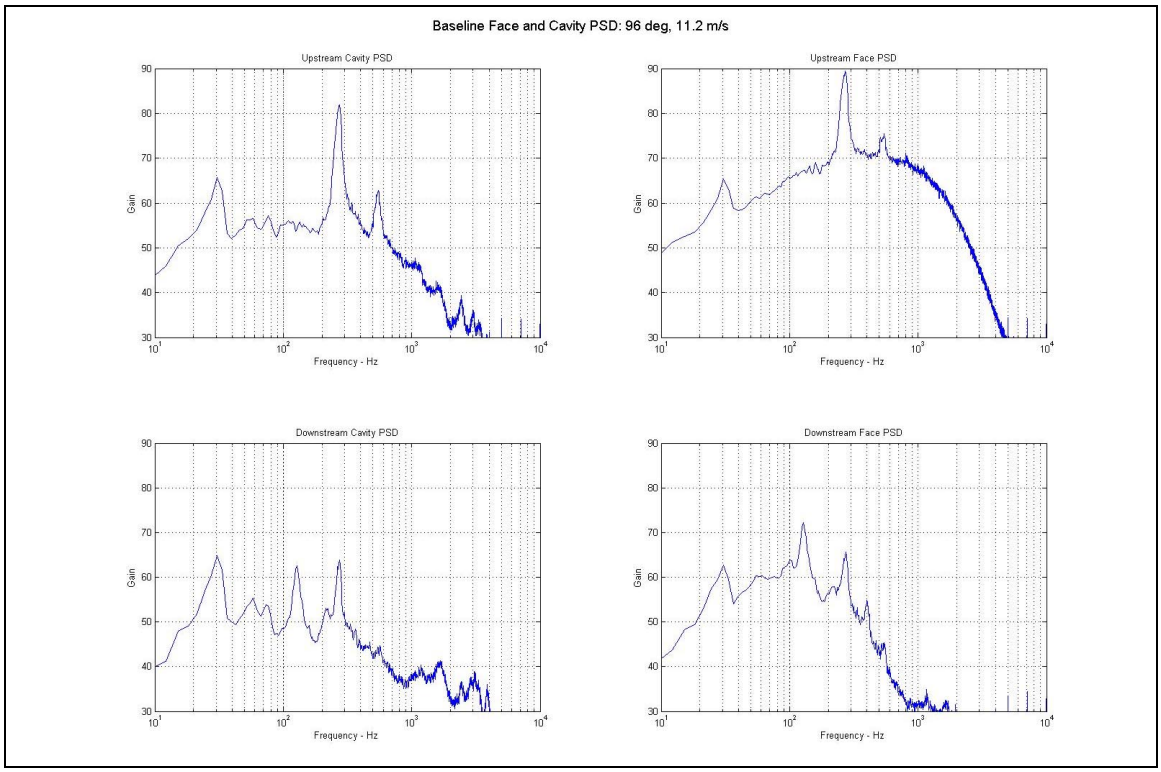

Figure 51. Face and Cavity Spectra, Slots Open, 11 m/s 96 deg

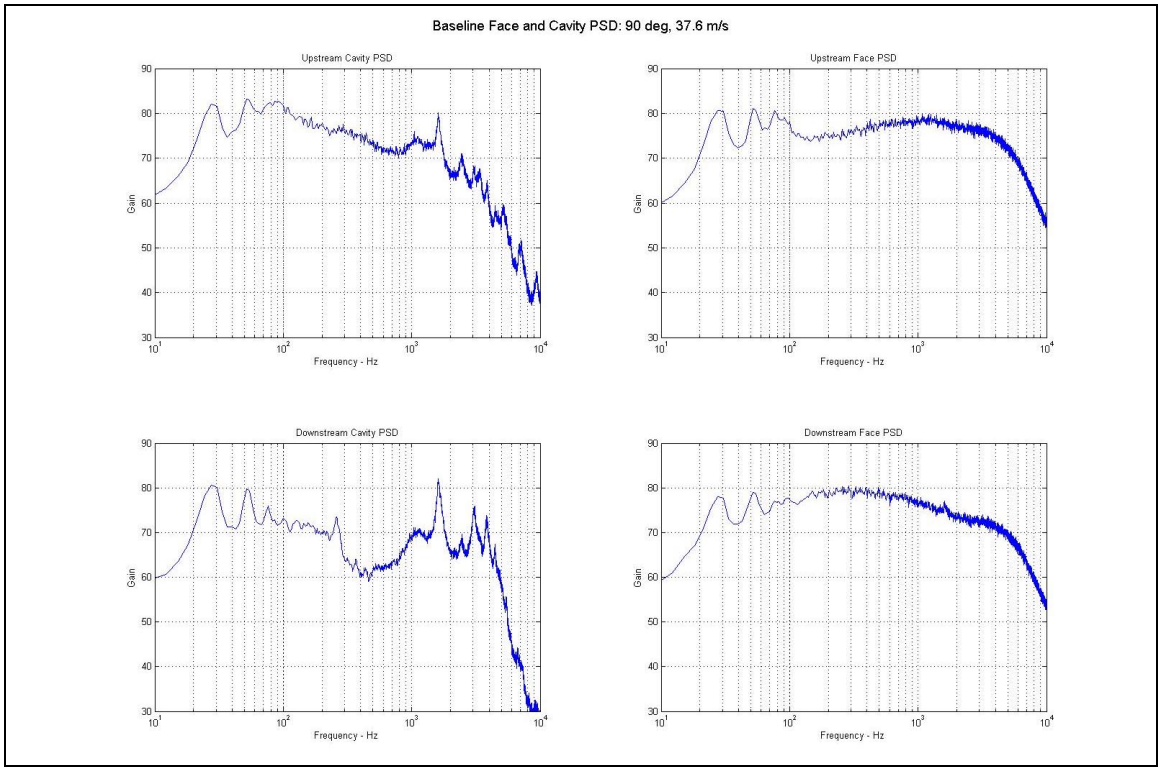

Figure 52. Face and Cavity Spectra, Slots Open, 37.6 m/s 90 deg

The two cavity pressure spectra from Figure 51 can be compared to results obtained early in the program, as shown in Figure 3 and recast in the upstream and downstream spectra of Figure 53. The frequency range is 200 Hz to 4 kHz. Note that the spectra are essentially similar to the post-modification results, but that the 1700 Hz peaks are sharper and higher by a few dB relative to the surrounding broadband noise. This may be further evidence of the stagger tuning effect of varied slot sizes.

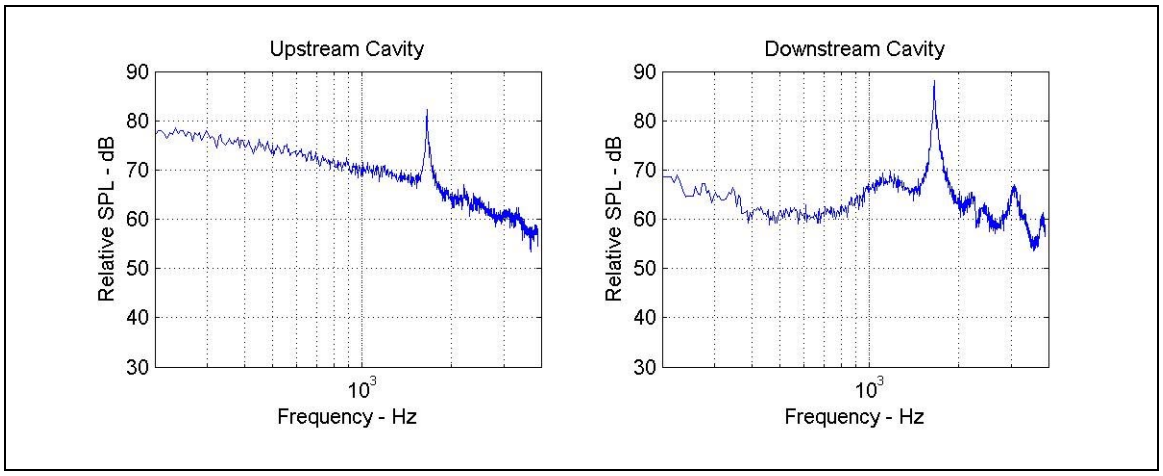

Figure 53. Pre-Slot Modification Spectra Measured in Upstream and Downstream Cavities for Comparison to Figure 51. Vinf = 37.6 m/s, Incidence Angle 90°.

Conclusions

1. Shear layer oscillations over flowliner slot cascades exposed to simulated swirl conditions for 104.5% operating point occurred at lower frequency (Nst ≈ 0.15 at Upstream slots) than would be supported by duct or cavity resonances in the flowliner. The amplitude of the pressure differential across the slot webbing was on the order 80 dB or 0.2 Pa rms.
2. Modification of single and multiple Upstream slots by elongating and modest side-grinding influenced the frequency and apparent amplitude of the shear layer oscillations, as determined from measurements of differential tone pressures across the central slot webbing in the 2D model. The tone pressure variation with modification depended upon flow speed and angle. Oscillation frequencies were generally reduced slightly as slots were increased in overall size, but the overall change was very small and in some cases the apparent result of separating multiple spectral peaks. At the lowest flow speed tested (7 m/s) amplitude increases of up to 51% and amplitude reductions of up to 31% were observed. At the higher speed (11.2 m/s) the range of change was only -24% to +18%.
3. When exposed to flow more nearly simulating swirl conditions at lower power operating point (31 – 37 m/s at 90-105 angle), significant response was obtained in upstream and downstream liner segments at frequency 1500-1700 Hz. Taping the upstream slots preserves this oscillation. Taping the downstream slots extinguishes it. Measurement of upstream and downstream cavity gains showed that the frequency range of this resonance corresponds to a resonance in the downstream liner segment.
4. Comparison of the higher swirl response of the flowliner segment with upstream slots significantly modified vs preliminary baseline conditions indicated a reduction is tone strength, suggesting that modifying upstream slots by crack grinding would not result in a higher tone generation potential at the lower power operating range.

Recommendations

1. On the basis of these test results, it does not appear that grinding/polishing upstream flowliner slots would significantly affect flowliner oscillations. Although the slot modifications increased oscillation pressures up to about 50% in some instances, the frequency of these oscillations was too low to couple well with expected duct or cavity resonance modes, as would be required to cause high level edge tone response.
2. The tests showed a potential for downstream slots to interact with liner acoustic resonance modes at higher swirling velocity conditions. Here, it may be possible that slot geometry changes could upset a loss-gain balance and trigger a strong oscillatory response. Further, the downstream slots are smaller than the upstream slots, so modifications would have a greater relative impact on their potential acoustical effects. If additional testing is to be done, it is recommended that similar parametric tests of systematic changes in slot geometry be undertaken.

REPORT DOCUMENTATION PAGE

Form Approved
OMB No. 0704-0188

1. AGENCY USE ONLY (*Leave blank*)	2. REPORT DATE	3. REPORT TYPE AND DATES COVERED
	December 2004	Final Contractor Report

4. TITLE AND SUBTITLE

Two-Dimensional Air-Flow Tests of the Effect of ITA Flowliner Slot Modification by Grinding/Polishing on Edge Tone Generation Potential

5. FUNDING NUMBERS

WBS–22–104–08–41
S40405

6. AUTHOR(S)

Bruce E. Walker

7. PERFORMING ORGANIZATION NAME(S) AND ADDRESS(ES)

Hersh Walker Acoustics
780 Lakefield Road, Unit G
Westlake Village, California 91361

8. PERFORMING ORGANIZATION REPORT NUMBER

E–14915

9. SPONSORING/MONITORING AGENCY NAME(S) AND ADDRESS(ES)

National Aeronautics and Space Administration
Washington, DC 20546–0001

10. SPONSORING/MONITORING AGENCY REPORT NUMBER

NASA CR—2004-213405

11. SUPPLEMENTARY NOTES

Project Manager, Daniel L. Sutliff, Structures and Acoustics Division, NASA Glenn Research Center, organization code RTA, 216–433–6290.

12a. DISTRIBUTION/AVAILABILITY STATEMENT

Unclassified - Unlimited
Subject Category: 18 Distribution: Nonstandard

Available electronically at http://gltrs.grc.nasa.gov

This publication is available from the NASA Center for AeroSpace Information, 301–621–0390.

12b. DISTRIBUTION CODE

13. ABSTRACT ***(Maximum 200 words)***

Hersh Walker Acoustics (HWA) has performed a series of wind tunnel tests to support crack-repair studies for ITA flowliner vent slots. The overall goal of these tests is to determine if slot shape details have a significant influence on the propensity of the flowliner to produce aero-acoustic oscillations that could increase unsteady stresses on the flowliner walls. The test series, conducted using a full-scale two-dimensional model of a six-slot segment of the 38 slot liner, was intended to investigate the effects of altering slot shape by grinding away cracked portions.

14. SUBJECT TERMS

Flowliner; Space Shuttle Main Engine

15. NUMBER OF PAGES

47

16. PRICE CODE

17. SECURITY CLASSIFICATION OF REPORT	18. SECURITY CLASSIFICATION OF THIS PAGE	19. SECURITY CLASSIFICATION OF ABSTRACT	20. LIMITATION OF ABSTRACT
Unclassified	Unclassified	Unclassified	